sustainability

MDPI

Article

Ecosystem Service Value Decline Along a Coastal Gradient: Evidence from Zhoushan Island

Wei Mo [1,2,*], Fangning Wu [3], Yonghua Tan [1,2], Li Sun [1,2] and Degang Wang [1,2]

[1] Second Institute of Oceanography, Ministry of Natural Resources, Hangzhou 310012, China; tanyonghua@sio.org.cn (Y.T.); sunli@sio.org.cn (L.S.); wangdegang@sio.org.cn (D.W.)
[2] Key Laboratory of Ocean Space Resource Management Technology, Ministry of Natural Resources, Hangzhou 310012, China
[3] National Research Institute for Rural Electrification, Hangzhou 310012, China
* Correspondence: mowei@sio.org.cn

Abstract

This study investigates ecosystem service valuation on Zhoushan Island. Based on Landsat remote sensing images for 2000, 2010, and 2020 acquired through the Google Earth Engine (GEE) platform, six land use types are extracted using the Random Forest method. By integrating land use dynamic degree, transfer matrix, ecosystem service value (ESV) accounting, and five-level land–sea gradient zoning approaches, this study systematically analyzes the spatiotemporal evolution of land use and its effects on ESV over the 20-year period, and reveals the spatial differentiation pattern of land use change and ESV gains and losses along the land–sea gradient. The results indicate that from 2000 to 2020, water bodies and cultivated land on Zhoushan Island experienced continuous decline while construction land expanded rapidly, driven by policy regulation, urbanization, and industrial transformation. Localized coastal areas exhibited a typical chain conversion process of "water body → bare land → construction land," which is closely associated with reclamation and land reclamation activities. Regional ESV declined continuously, reaching only 56.7% of its 2000 level by 2020, with regulating and provisioning services exhibiting the most pronounced deterioration. Analysis of the ESV net transfer matrix indicates that the primary driver of ESV decline was the large-scale conversion of high-value water bodies to low-value construction land and bare land, the magnitude of which far exceeded the positive ecological gains generated by all other land use conversions. The reduction in cultivated land area, compounded by adjustments in cropping structure, has placed sustained pressure on regional food security, and policy responses have lagged considerably behind the pace of ecological degradation. In terms of spatial differentiation, both the intensity of land use change and ESV loss exhibited a gradient pattern that decreases progressively from the coastal zone moving inland. Zone 1 and Zone 2 in the nearshore area together accounted for approximately 80% of total ESV loss, whereas Zone 4 and Zone 5 maintained relatively stable land use structures and ecological support capacity, owing to higher forestland coverage. Spearman's rank correlation analysis confirmed a statistically significant monotonically decreasing relationship between land use dynamic degree and coastal distance. Policy regulation served as the primary driver of regional land use pattern evolution: early sea reclamation policies facilitated rapid land transformation along the coastline, while subsequent tightening of controls effectively curbed disorderly expansion.

Keywords: ecosystem service value; land use change; Zhoushan Island; Google Earth Engine; land–sea gradient; coastal reclamation; spatiotemporal analysis

Check for updates

Academic Editor: Chaoqun Wang

Received: 7 April 2026
Revised: 28 May 2026
Accepted: 31 May 2026
Published: 3 June 2026

Copyright: © 2026 by the authors. Licensee MDPI, Basel, Switzerland. This article is an open access article distributed under the terms and conditions of the Creative Commons Attribution (CC BY) license.

1. Introduction

Land use/cover change (LUCC) is a frequently studied topic in global and regional environmental change studies, highlighting how land use change reflects the interaction between people and the environment [1]. Land use changes alter ecosystem functions and structures, leading to increases or decreases in ecosystem service value (ESV) [2–5], and are often driven by natural processes or human activities. The latter are often the primary reason for changes in ESV, particularly in urban areas [6,7].

Ecosystem service value is the sum of the tangible and intangible benefits that humans obtain from ecosystems [8]. Furthermore, ecosystem services are crucial for sustaining life on Earth, maintaining ecosystem integrity, and supporting sustainable development [9,10]. Costanza initially outlined principles and methods for evaluating ecosystem service value [9,11], laying the groundwork for quantitative assessment. In recent years, ecosystem service valuation techniques have been continually refined and enhanced [11,12], and Xie et al. developed a China-specific method for assessing ecosystem service value, tailored to the country's ecosystem features and based on Costanza's model [13–15].

According to the classic Theory of Island Biogeography proposed by MacArthur and Wilson (1967), islands are not simply landmasses surrounded by seawater, but rather independent ecosystems with unique evolutionary and successional mechanisms [16,17]. Constrained by limited land area, isolated geographical location, and relatively homogeneous habitat structure, island ecosystems support smaller population sizes and narrower survival thresholds than continental areas, making them highly sensitive to human disturbances such as urbanization. Once disturbed, native species are more vulnerable to extinction, and geographical isolation greatly impedes natural recolonization following habitat degradation, resulting in a self-recovery capacity far weaker than that of interconnected continental habitat patches. Consequently, island ecosystems have very limited ecological margins for planning errors and require precise assessment and spatial regulation.

Current island-related research spans multiple fields, including biogeography [18,19], tourism [20,21], and sustainable development [22,23], and has revealed the vulnerability and complexity of island ecosystems from different dimensions. However, gradient analyses conducted from a land–sea interaction perspective remain relatively rare.

As the primary interface of between land and sea interaction, the coastline experiences the most intense human activity and is itself a dynamic boundary whose long-term position is modulated by sediment supply, beach-face morphology, and storm forcing. Multi-decadal analyses of satellite-derived shorelines further demonstrate that erosion–accretion asymmetries and beach-face steepness exert measurable control on coastal vulnerability and disaster risk patterns at the transect scale [24,25], reinforcing the rationale for explicitly resolving coastal gradients in island ecosystem service value assessments. Generally, areas closer to the shoreline face greater ecological disturbance pressures, with land development intensity gradually diminishing from the coast inland [26–28]. Owing to their small area, low ecological thresholds, and highly concentrated human activities, islands exhibit steeper land–sea gradients and more sensitive ecological responses.

Recent research has predominantly focused on the ecological effects of land use change, emphasizing the spatiotemporal dynamics of ESV [29,30]. However, studies conducting gradient analyses of island ecosystems from a land–sea interaction perspective remain relatively scarce, limiting the applicability of research findings in guiding precise spatial management and ecological conservation strategies for islands. Maintaining ecosystem service functions and resource supply capacity while ensuring economic development and urban expansion has become a core challenge for sustainable island development.

As China's fourth largest island and the core area of the first prefecture-level city established under an archipelago administrative system, Zhoushan Island has undergone

rapid urbanization since the establishment of the Archipelago New Area in 2011 [31]. However, the tension between relative land scarcity and sustained development demand has become increasingly apparent, and intensive coastal development activities, while driving economic growth, have also exerted non-negligible impacts on the long-term sustainability of ecosystems. Existing ESV studies on Zhoushan have mostly adopted year-by-year dynamic shorelines, which can reflect overall regional ecological evolution. However, when quantifying the net ecological losses from coastal development activities, the total study area expands progressively with reclamation, and the low ecological value of newly added artificial land dilutes the ecological losses of the original sea areas. The seaward advance of the Zhoushan Island shoreline from 2000 to 2020 was driven primarily by coastal development activities, with natural sedimentation and erosion processes contributing negligibly. In light of this, this study adopts the 2020 coastline as a unified spatial baseline to ensure a constant total study area and longitudinal comparability of gradient analysis.

Although previous studies have explored land use and ecosystem service changes in the Zhoushan Archipelago [32–37], analyses based on coastal gradient and multi-zone spatiotemporal differentiation remain relatively weak. To address this gap, this study systematically analyzes the land–sea gradient characteristics of land use on Zhoushan Island and explores the spatiotemporal relationship between land use and ecosystem service value, leveraging the Google Earth Engine (GEE) cloud platform and multi-temporal Landsat imagery spanning 2000 to 2020. This study aims to examine the influence of human–environment interactions on land use change along the land–sea gradient of Zhoushan Island, assess the sustainability of island ecosystem services under intensive development, and reveal the spatiotemporal differentiation patterns and driving mechanisms of ESV across different zones, thereby providing a scientific basis for island spatial management and ecological conservation.

2. Materials and Methods

2.1. Study Area

Zhoushan Island is the largest in Zhejiang Province, located in the middle of China's eastern coastline in the East China Sea, off the northeastern coast of Zhejiang (Figure 1), and is the main island of the Zhoushan Archipelago, as shown in Figure 1. The central and western regions of Zhoushan Island are part of the Dinghai District; in contrast, the eastern region belongs to the Putuo District. Benefiting from fertile soil and well-developed water systems, Zhoushan plays a vital role in water conservation and is a key center for forestry resources within Zhoushan City.

In recent years, Zhoushan Island has undergone rapid urbanization due to the ongoing growth of ocean-related industries [38], which has involved expanding urban areas, building transportation infrastructure, and meeting the rising need for industrial land. Combined with limited island land resources, these factors have resulted in extensive land reclamation from water bodies and tidal flats, as well as the transformation of farmland into developed land.

2.2. Methods

2.2.1. Land Use Extraction

In this study, land use data for Zhoushan Island were extracted using the GEE platform, and the extraction methodology is shown in Figure 2. GEE can be effectively applied across various Earth Science studies, including Land Use Change Monitoring [39], Coastline Change [40], Marine Aquaculture Area changes [41,42], and Marine Disaster Monitoring [43].

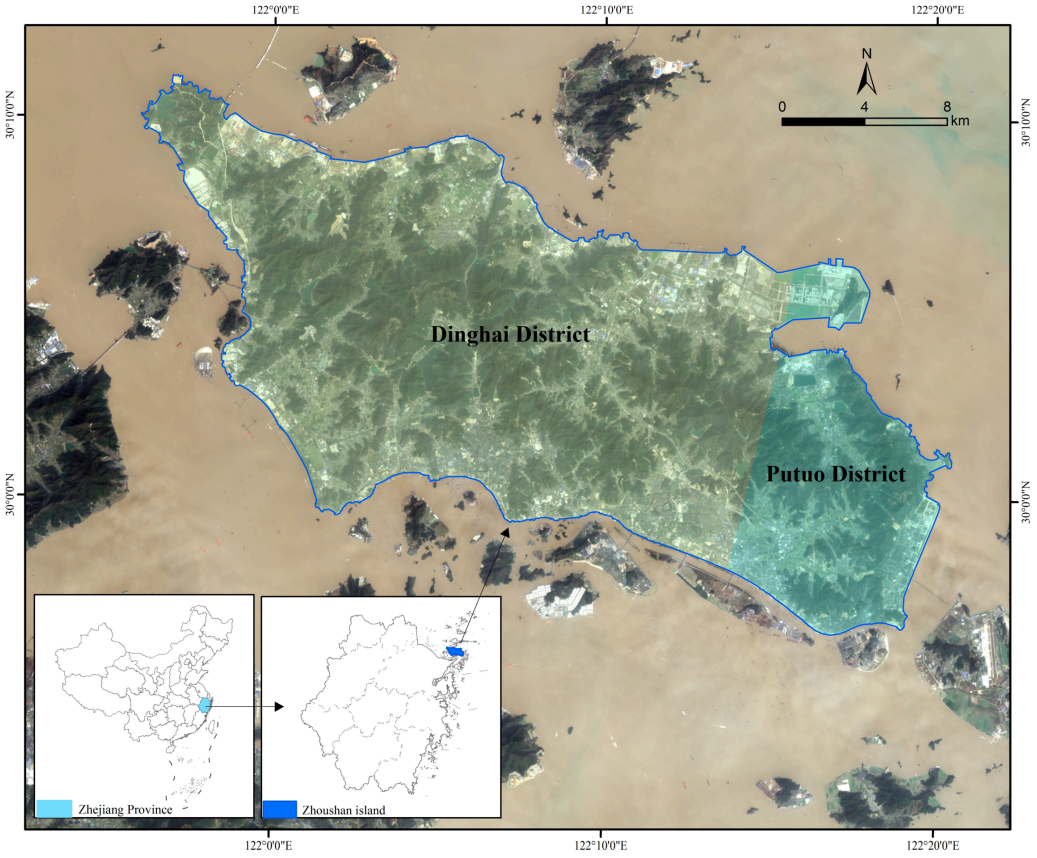


Figure 1. Geographic location of Zhoushan Island. In the two inset maps, light blue represents Zhejiang Province and dark blue denotes Zhoushan Island. The two black arrows guide the reader's view from the national overview map, to the provincial extent, and finally to the main study area.

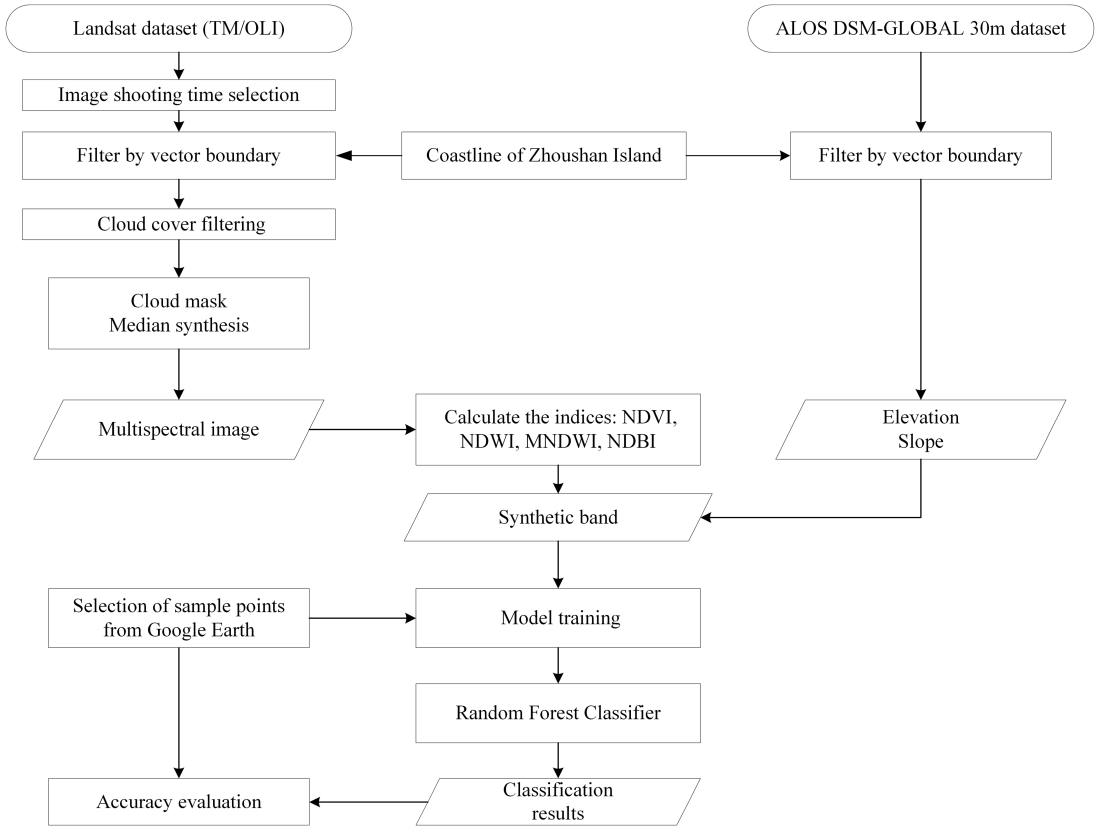


Figure 2. The flowchart mapping land use extraction on the GEE platform.

The remote sensing data included Landsat 5 SR data (LANDSAT/LT05/C02/T1_L2) for 2000 and 2010, Landsat 8 SR data (LANDSAT/LC08/C02/T1_L2) for 2020, and the ALOS DSM-GLOBAL 30 m dataset with a spatial resolution of 30 m.

(1) Sample point selection

Referring to the National Land Cover Dataset of China [44] and based on the actual conditions of Zhoushan Island, six land cover types were used in this study: farmland, forest, grassland, water, construction land, and barren land.

The sampling and validation scheme of this study followed the method of Nasiri et al. [45]. All samples were obtained through visual interpretation of high-resolution Google Earth imagery, using a random polygon-based sampling strategy. The sample proportions were generally consistent with the area of each land use type, and the spatial distribution of samples was even. The total sample set was split into two parts: 70% for the training dataset and 30% for the verification dataset.

(2) Remote sensing image processing

Landsat remote sensing data from April to September, corresponding to the vegetation growing season of the year, were filtered based on cloud cover, and images with cloud coverage below 10% were retained. After applying a cloud removal function, median compositing was performed, and the result was then clipped using the island vector boundary.

(3) Multiband composition

To enhance extraction accuracy, several widely used index bands were used, namely the Normalized Difference Vegetation Index (NDVI) [46], modified Normalized Difference Water Index (mNDWI) [47,48], and Normalized Difference Built-up Index (NDBI) [49].

The formulas for these indices are as follows:

$$\mathrm{NDVI} = \frac{NIR - Red}{NIR + Red} \tag{1}$$

$$\mathrm{mNDWI} = \frac{Green - SWIR}{Green + SWIR} \tag{2}$$

$$\mathrm{NDBI} = \frac{SWIR - NIR}{SWIR + NIR} \tag{3}$$

Here, *Green*, *Red*, *NIR*, and *SWIR* are the bands of Landsat TM/OLI imagery, corresponding to green (520–600 nm), red (630–690 nm), near-infrared (760–900 nm), and shortwave infrared (1550–1750 nm), respectively.

The composite NDVI, mNDWI, NDBI, DEM and slope (both from the GEE SRTM dataset), and multiple Landsat bands were used to perform classification with the stochastic forest method.

(4) Land use classification accuracy verification

OA and kappa indices were used to verify the accuracy of the classification data, and the results are shown in Table 1. The complete confusion matrices for each year are provided in Supplementary Table S1. Due to the similarity of spectral signatures among certain land cover types, minor confusions were observed primarily between construction land and barren land, as well as between construction land and farmland. Grassland also exhibited noticeable omission in certain years. Nevertheless, the overall accuracy (OA) and kappa coefficients for all three periods remained at high levels.

2.2.2. Calculation of ESV

Ecosystem services include provisioning, regulating, supporting, and cultural services. Based on the Costanza method [13–15], a questionnaire survey was conducted among

domestic ecological experts, and a unit value system for ecosystem services tailored to China's conditions was developed. In this study, the equivalent value factor conversion method proposed by Xie was applied and the equivalence table was customized according to the specific conditions of the study area. Referencing relevant research [50], the equivalent value for construction land was set to 0. Furthermore, the barren land in this study predominantly consists of transitional bare surfaces formed by coastal reclamation around Zhoushan Island. These surfaces were created through the construction of cofferdams, hydraulic filling of dredged sediment, and foundation reinforcement techniques, representing highly disturbed artificial ground. This type of land surface lacks tidal hydrological processes, natural wetland structure, and vegetation or biological communities; it does not constitute natural tidal flats or coastal wetlands; and its ecosystem service functions are extremely weak. Referring to previous studies conducted in Zhoushan and Zhejiang Province [37,50], the desert ecological value coefficient was assigned to this type of barren land to reflect its actual level of ecological function.

Table 1. Interpretation accuracy statistics.

Year	OA	Kappa
2000	98.6%	98.0%
2010	98.7%	98.4%
2020	96.2%	94.9%

The main grain crop in Zhoushan City is late-season rice. Using data from the Zhoushan City Statistical Yearbook, including the sown area, yield, and average price of late-season rice in 2020, the per-unit-area economic output of grain production on Zhoushan's farmland can be approximated. This total is then divided by 7 to derive the value of one ecosystem service equivalent, approximately 3383.33 yuan per hectare, which was used to create a table of ecosystem service value coefficients for various land types on Zhoushan Island, detailed in Table 2.

Table 2. Ecosystem service value coefficient of the study area (Unit: yuan/hm^2).

Level 1	Level 2	Farmland	Forest	Grassland	Water	Construction Land	Barren Land
Provisioning services	Food production	3755.50	845.83	778.17	2706.67	0.00	33.83
	Material	845.83	1962.33	1150.33	778.17	0.00	101.50
	Water supply	−4432.17	1015.00	642.83	28,047.84	0.00	67.67
Regulating services	Gas regulation	3011.17	6462.17	4093.84	2605.17	0.00	372.17
	Climate regulation	1590.17	19,318.84	10,792.84	7747.84	0.00	338.33
	Environment purification	473.67	5650.17	3552.50	18,777.51	0.00	1048.83
	Water regulation	5075.00	12,653.67	7917.00	345,912.13	0.00	710.50
Supporting services	Soil conservation	1759.33	7849.34	4973.50	3146.50	0.00	439.83
	Nutrient cycling	541.33	609.00	372.17	236.83	0.00	33.83
	Biodiversity	575.17	7172.67	4533.67	8627.50	0.00	406.00
Cultural services	Esthetic landscape	270.67	3146.50	1996.17	6394.50	0.00	169.17
Total		13,465.67	66,685.52	40,803.02	424,980.66	0.00	3721.66

2.2.3. ESV Sensitivity Analysis

To verify the reliability of the ESV assessment results, the coefficient of sensitivity (CS) method was employed for validation [51]. The value coefficients per unit area for farmland, forest, grassland, water bodies, and barren land were individually adjusted upward and downward by 50%, while those of the other land use types remained unchanged. The total ESV was then recalculated, and the corresponding CS was derived using the following formula:

$$CS = \left| \frac{(ESV_j - ESV_i)/ESV_i}{(VC_{jk} - VC_{ik})/VC_{ik}} \right| \quad (4)$$

where ESV_i and ESV_j represent the total ecosystem service value before and after adjustment, respectively; VC_{ik} and VC_{jk} represent the value coefficient per unit area of a given land use type before and after adjustment, respectively.

2.2.4. Land Use and ESV Change Analysis

(1) Land use change state degree

The single land use dynamic rate indicates how a specific land use type changes over the study period and is calculated by the following formula:

$$K = \frac{U_b - U_a}{U_a} \times \frac{1}{T} \times 100\% \quad (5)$$

where K denotes the land use dynamic degree for a given land use type over the study period, U_a and U_b represent the area of that land use type at the initial and final time points, respectively, and T is the duration of the study in years.

(2) Comprehensive dynamic degree

The comprehensive dynamic degree of land use refers to the rate of change in overall land use types during the study period, and the calculation formula is as follows:

$$LC = \left[\frac{\sum_{i=1}^{n} \Delta LU_{i-j}}{2\sum_{i=1}^{n} LU_i} \right] \times \frac{1}{T} \times 100\% \quad (6)$$

where LC denotes the comprehensive land use dynamic degree over the study period; ΔLU_i denotes the area of land use i at the beginning of the study period; $\Delta LU_{i\text{-}j}$ is the absolute area converted from type i to other land use types during the study interval; n is the total number of land use categories; and T is the study duration in years.

(3) Land use and ESV Change transition matrix

The land use transition matrix is used to describe the direction and quantity of land use type changes during the study period [52], calculated as follows:

$$U_{xy} = \begin{bmatrix} U_{11} & U_{12} & \cdots & U_{1n} \\ U_{21} & U_{22} & \cdots & U_{2n} \\ \cdots & \cdots & \cdots & \cdots \\ U_{n1} & U_{n2} & \cdots & U_{mn} \end{bmatrix} \quad (7)$$

where Uxy is the conversion of land use type x at the beginning of the study to land use type y at the end of the study, measured as land area. On this basis, we constructed an ESV transfer matrix to quantify the ESV variation induced by the transformation from land type x to y, where Uxy represents the ESV change derived from the land area converted between the two types.

2.2.5. Island Zoning Method

In coastal research, zoning the study area by distance from the shoreline is a common approach [51]. To characterize the spatial attenuation features of human activity disturbances, the natural breaks method was applied in this study to divide Zhoushan Island along the land–sea gradient, as it maximizes inter-group differences and minimizes intra-group differences, demonstrating strong applicability. Based on the Euclidean distance from the center point of each 500 m grid to the coastline, the study area was divided into five gradient zones from near to far, namely Zone 1 (nearshore) to Zone 5 (offshore),

thereby enabling a standardized comparative analysis of the land use pattern and the spatial differentiation of ecosystem services. Spatial zoning, distance calculation and corresponding cartographic production were performed in ArcGIS 10.8 (Esri, Redlands, CA, USA) (Figure 3).

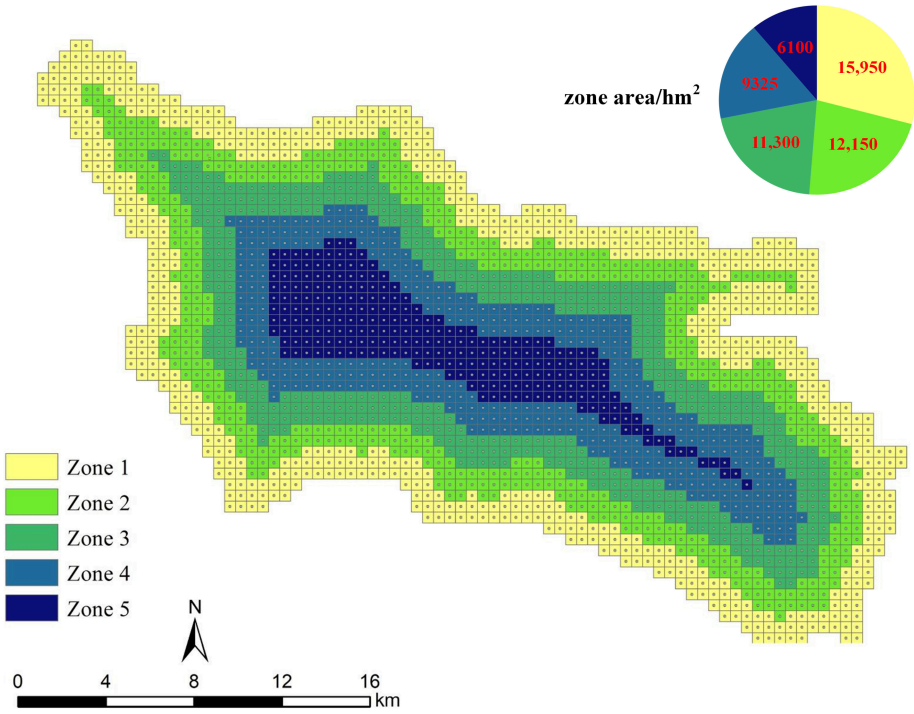


Figure 3. Zoning map and area statistics chart of Zhoushan Island.

To assess the potential influence of the Modifiable Areal Unit Problem (MAUP)—a common issue in spatial analysis—on the conclusions [53–55], this study introduced two additional zoning schemes with three and seven zones, respectively, for robustness testing. The MAUP refers to the phenomenon whereby the results of spatial analysis vary depending on how the basic spatial units are defined (e.g., their scale or boundaries). By comparing the spatial patterns of ESV loss rates across the three zoning schemes, the sensitivity of the core conclusion to the number of zones could be evaluated: if the core pattern of "ESV loss highly concentrated in nearshore zones" remains stable across different zoning schemes, this indicates that the conclusion is robust and not dominated by the choice of the number of zones.

In addition, to test the statistical significance of the variation in land use intensity with distance from the coast, Spearman's rank correlation analysis was employed to examine the monotonic relationship between land use dynamic degree and coastal distance. This method is a nonparametric test that does not depend on assumptions about data distribution, making it suitable for statistical inference of monotonic trends under small-sample conditions.

3. Results

3.1. Overall Analysis

3.1.1. Spatial–Temporal Evolution and Dynamics of Land Use

Table 3 and Figure 4 present the land use dynamics of Zhoushan Island from 2000 to 2020. Forestland constituted the predominant land cover throughout the study period, followed by farmland and construction land. Substantial changes were detected in farmland, water bodies, construction land, and barren land. Between 2000 and 2020, farmland steadily decreased from 14,053.78 hm^2 to 10,277.42 hm^2, with an average annual change

rate of −1.34%; forest showed a minor decrease from 26,965.44 hm^2 to 25,465.88 hm^2, at the same average annual rate of −1.34%; and water bodies continuously declined from 5369.91 hm^2 to 1308.57 hm^2, at an average annual rate of −3.78%. However, construction land increased significantly from 5135.56 hm^2 to 13,369.47 hm^2; between 2000 and 2010 alone, this area grew by 5286.4 hm^2, with an overall growth rate of 8.02% over the 20 years.

Table 3. Land use types and area changes (unit/hm^2).

Year	Farmland	Forest	Grassland	Water	Construction Land	Barren Land	Total Area
2000	14,053.78	26,965.44	151.73	5369.91	5135.56	432.13	52,108.55
2010	10,614.75	25,162.17	368.98	4024.36	10,421.96	1516.33	
2020	10,277.42	25,465.88	679.81	1308.57	13,369.47	1007.4	

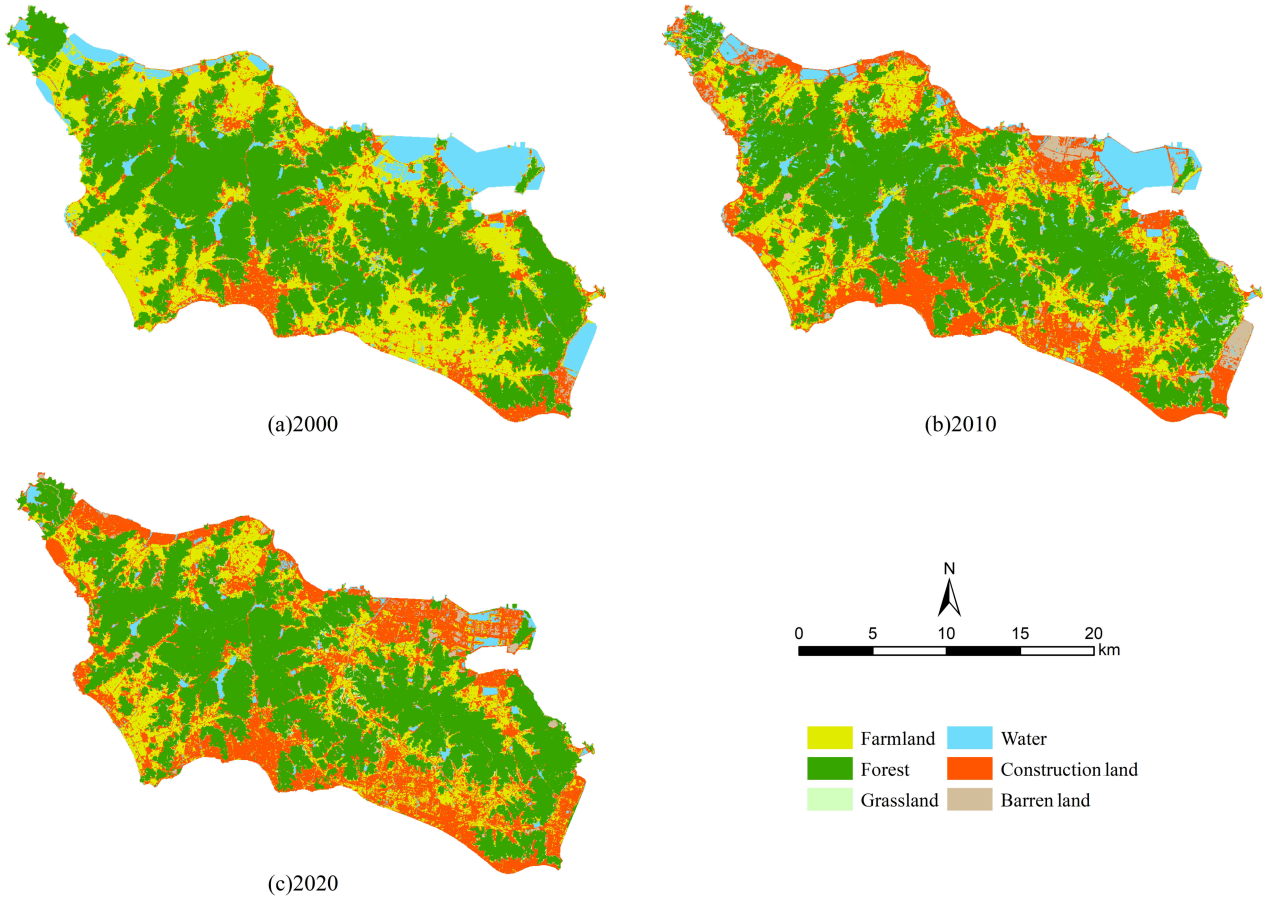


Figure 4. Land use patterns on Zhoushan Island from 2000 to 2020.

Similarly, unused land increased significantly, rising from 432.13 hm^2 to 1007.4 hm^2; this growth was especially notable between 2000 and 2010, with an average annual growth rate of 25.09% and an overall increase of 6.66%.

The Sankey diagram (Figure 5) derived from the land transfer matrix reveals that between 2000 and 2020, forestland continually exchanged land with other types. Meanwhile, farmland steadily decreased and was mostly converted to construction land, with its proportion of the total area falling from 26.97% to 19.72%, a reduction of 3776.36 hm^2.

Over 20 years, water areas shrank by 4061.34 hm^2, representing 75% of their 2000 size, and were mostly turned into construction land and barren land, with areas of 3140.97 hm^2 and 313.03 hm^2, respectively. The most significant decline occurred between 2010 and 2020, when 2715.79 hm^2 was lost, including 1396.67 hm^2 converted to construction land.

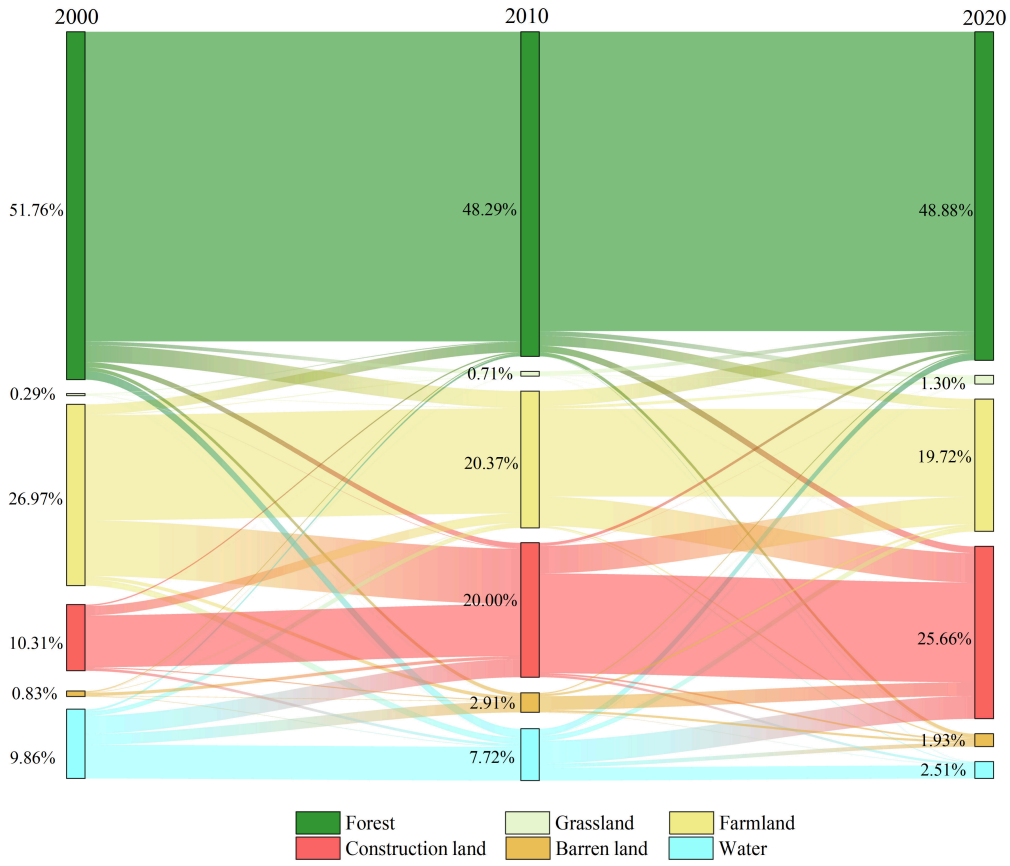


Figure 5. Sankey diagram of the conversion of each land use type from 2000 to 2020.

Construction land underwent sustained expansion, with its proportion of the total area rising from 9.86% to 25.66%, an increase primarily stemming from farmland, water, and forestland. There has also been a persistent two-way conversion between farmland and forestland: between 2000 and 2010, most conversions were from forestland to farmland; however, from 2010 to 2020, the trend shifted, with slightly more farmland being converted to forestland than the reverse.

3.1.2. Changes in Ecosystem Service Value

As illustrated in Figure 6, the overall ESV of the study area was 42,773.54 $\times$ 10^5 yuan in 2000, 35,518.64 $\times$ 10^5 yuan in 2010, and 24,242.04 $\times$ 10^5 yuan in 2020, showing a continuous downward trend over the past two decades. It declined by 7254.90 $\times$ 10^5 yuan between 2000 and 2010 and further fell by 11,276.60 $\times$ 10^5 yuan from 2010 to 2020; by 2020, the ESV had dropped to 56.7% of its 2000 level. Forestland, water bodies, and farmland made up the main components of the total ESV. Forestland contributed over 42% of the total ESV in each of the three periods, with both the absolute value and proportion remaining fairly stable. Water bodies experienced the most significant decline, decreasing from 22,821.07 $\times$ 10^5 yuan in 2000 to 5561.19 $\times$ 10^5 yuan in 2020, with their share dropping from 53% to 23%. Although the ESV of farmland declined from 1892.43 $\times$ 10^5 yuan in 2000 to 1383.93 $\times$ 10^5 yuan in 2020, its proportion stayed relatively steady. Grassland and barren land contribute little to the total ESV. Therefore, barren land is excluded from Figure 6, as its proportion is so small that it cannot be meaningfully presented.

Temporal variations in the composition of ESV are reflected in the proportional changes in different ecosystem service functions (Figure 7). Regulatory functions were consistently the primary focus of the island ecosystem, accounting for over 70%, and support services were the second most significant, maintaining a steady share above 12%. Meanwhile,

provisioning and cultural services were smaller in proportion: cultural services remained relatively stable, whereas provisioning services declined by nearly 50%.

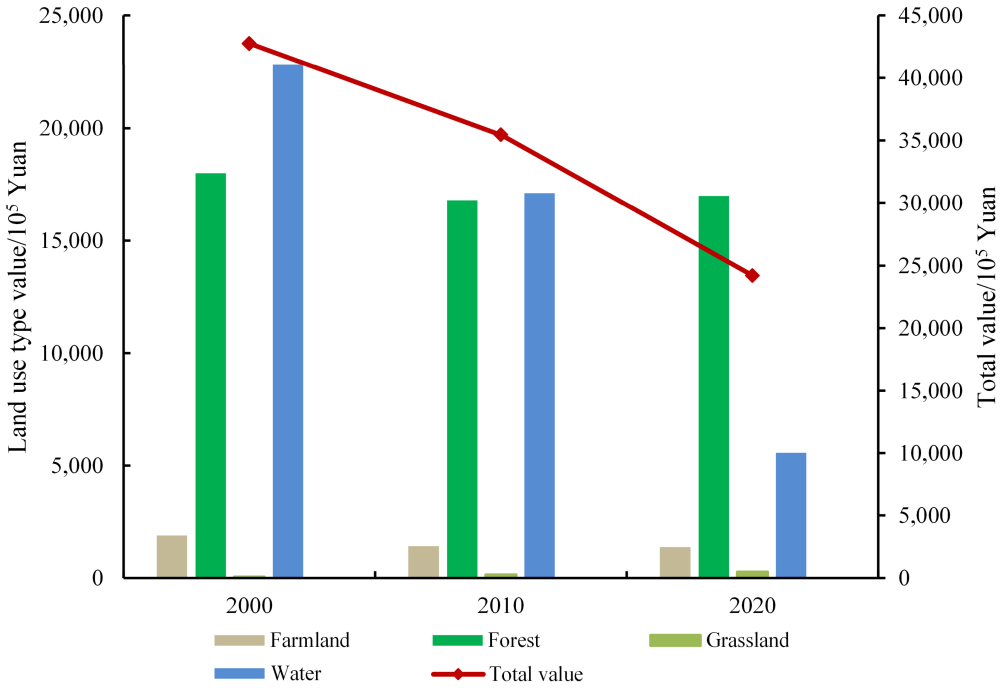


Figure 6. Total changes in ecosystem service value (ESV) from 2000 to 2020.

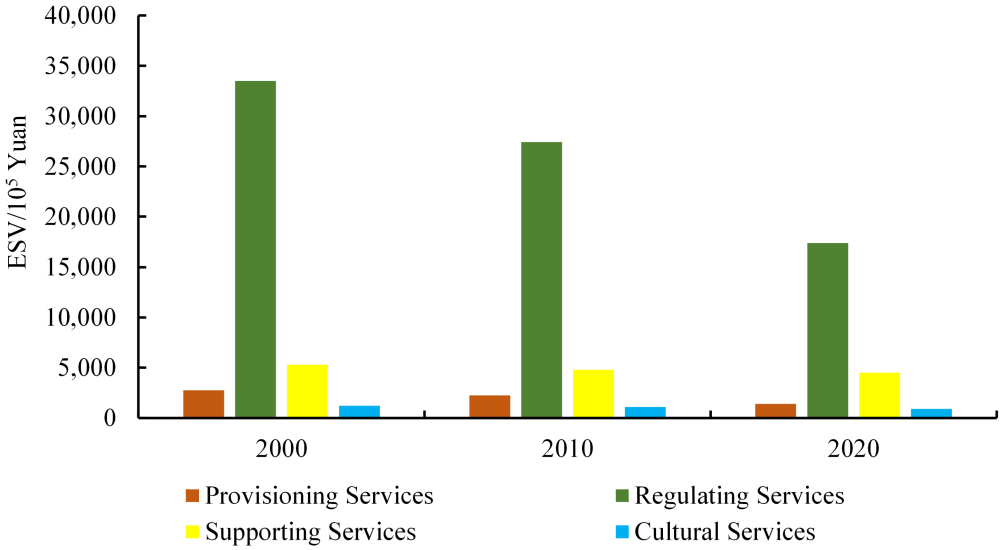


Figure 7. Individual ecosystem service value (ESV) from 2000 to 2020.

3.1.3. Results of ESV Sensitivity Analysis

The results of the ESV sensitivity analysis (Table 4) show that the sensitivity coefficients (CSs) for all land use types in all three years were far below 1, with the maximum value being 0.701 for forests in 2020. This indicates that the ESV estimates lack elasticity with respect to changes in the value coefficients of individual land use types, demonstrating that the research conclusions are robust and not dominated by the setting of any single coefficient.

Although water bodies were the core driver of ESV loss, their CS decreased from 0.534 in 2000 to 0.229 in 2020, indicating that, with the sharp reduction in water area, the influence of changes in the water coefficient on the total ESV weakened considerably. In contrast, the CS for forestland increased from 0.420 in 2000 to 0.701 in 2020 because forests

became the largest contributor to total ESV (accounting for 70%) following the substantial shrinkage of the water area. Nevertheless, its CS remained below 1, confirming that the results are still robust.

Table 4. The coefficient of sensitivity (CS) of ecosystem service value.

Land Use Type	2000	2010	2020
Farmland	0.044	0.04	0.057
Forest	0.42	0.472	0.701
Grassland	0.001	0.004	0.011
Water	0.534	0.482	0.229
Construction land	0	0	0
Barren land	0	0.002	0.002

3.1.4. ESV Net Transfer Matrix

The ESV net transfer matrices for the two periods were constructed (Figure 8, Table S2) to quantify the direction and magnitude of the contribution of each land use conversion to ecological value changes.

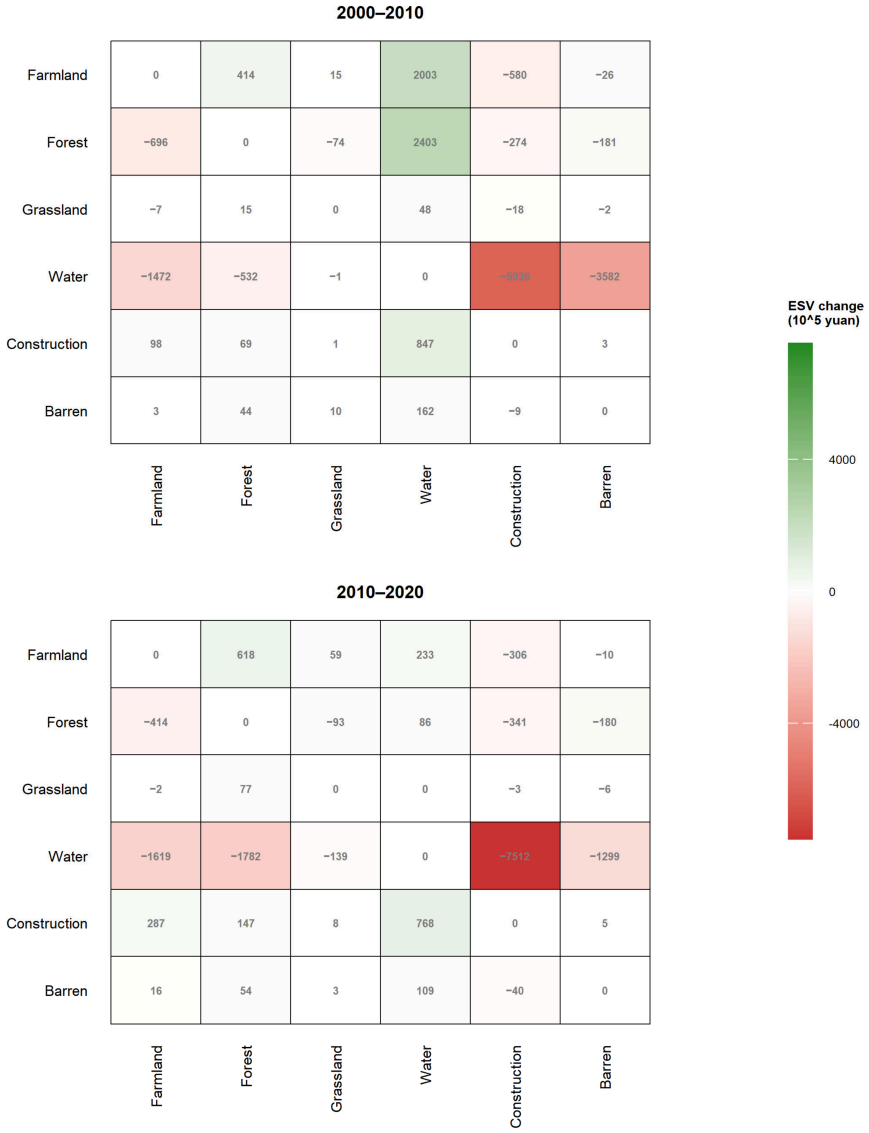


Figure 8. Ecosystem service value (ESV) net transfer matrix.

2000–2010: The net ESV loss originated primarily from the conversion of water bodies, as their transformation to construction land, barren land, and farmland resulted in net losses of 5935.56 × 10^5 yuan, 3582.18 × 10^5 yuan, 1471.63 × 10^5 yuan, respectively. These three pathways together accounted for 10,989.37 × 10^5 yuan, representing 95.4% of the total loss from water body conversion. Over the same period, the combined positive gains from forest and grassland conversions totaled only approximately 521.35 × 10^5 yuan, far from sufficient to offset the ecological value losses caused by the conversion of water bodies.

2010–2020: The value losses from water body conversion intensified further, with the combined net loss from their transformation to construction land, forest, farmland, and barren land amounting to 12,212.22 × 10^5 yuan. Although forest and grassland areas increased, their combined value gain was only approximately 916 × 10^5 yuan, equivalent to merely 7.5% of the losses from water body conversion, and thus unable to compensate for the aforementioned ecological value deficit.

The above results demonstrate that the core driving force behind the decline in ESV in the study area was the large-scale conversion of high-ecological-value water bodies to low-value construction land and barren land. The scale of these losses far exceeded the positive ecological gains generated by the conversion of other land use types, forming a pattern in which "high-value losses greatly outweigh low-value gains".

3.2. Gradient Differentiation of Spatiotemporal Changes

3.2.1. Gradient Differentiation of Spatiotemporal Changes in Land Use

Substantial heterogeneity in land use structure can be observed across the five subzones of Zhoushan Island. As illustrated in Figure 9, Zone 1 displayed a distinctly different land use pattern compared with the other zones. In 2000, it had considerably higher proportions of farmland, construction land, and water bodies, and it also underwent the most intense structural changes over time. For example, construction land in Zone 1 expanded rapidly from 2268 hm^2 in 2000 to 6115 hm^2 in 2020, contributing 47% of the island-wide increase in construction land. By contrast, Zones 2–5 exhibited similar land use structures, with much milder changes than Zone 1.

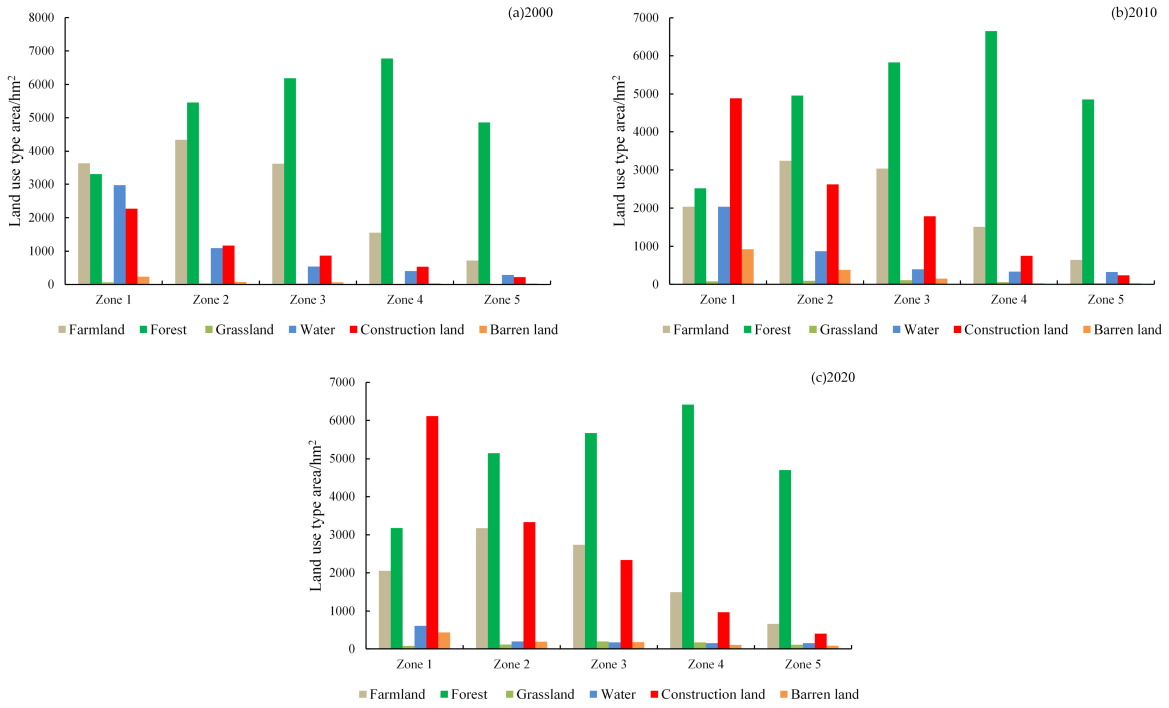


Figure 9. Land use structure of each zone in 2000, 2010, and 2020.

Figure 10 first examines the trends in farmland area. In 2000, Zone 2 had the largest share of farmland, followed by Zone 3 and Zone 4. Over the last twenty years, the total farmland area has diminished, especially between 2000 and 2010. During this period, Zone 1's farmland decreased from 3630 hm^2 to 2034 hm^2, with its share of Zone 1's total area dropping from 29% to 16%; likewise, Zone 2's farmland shrank from 4336 hm^2 to 3240 hm^2, and its share of Zone 2's total area fell from 36% to 27%.

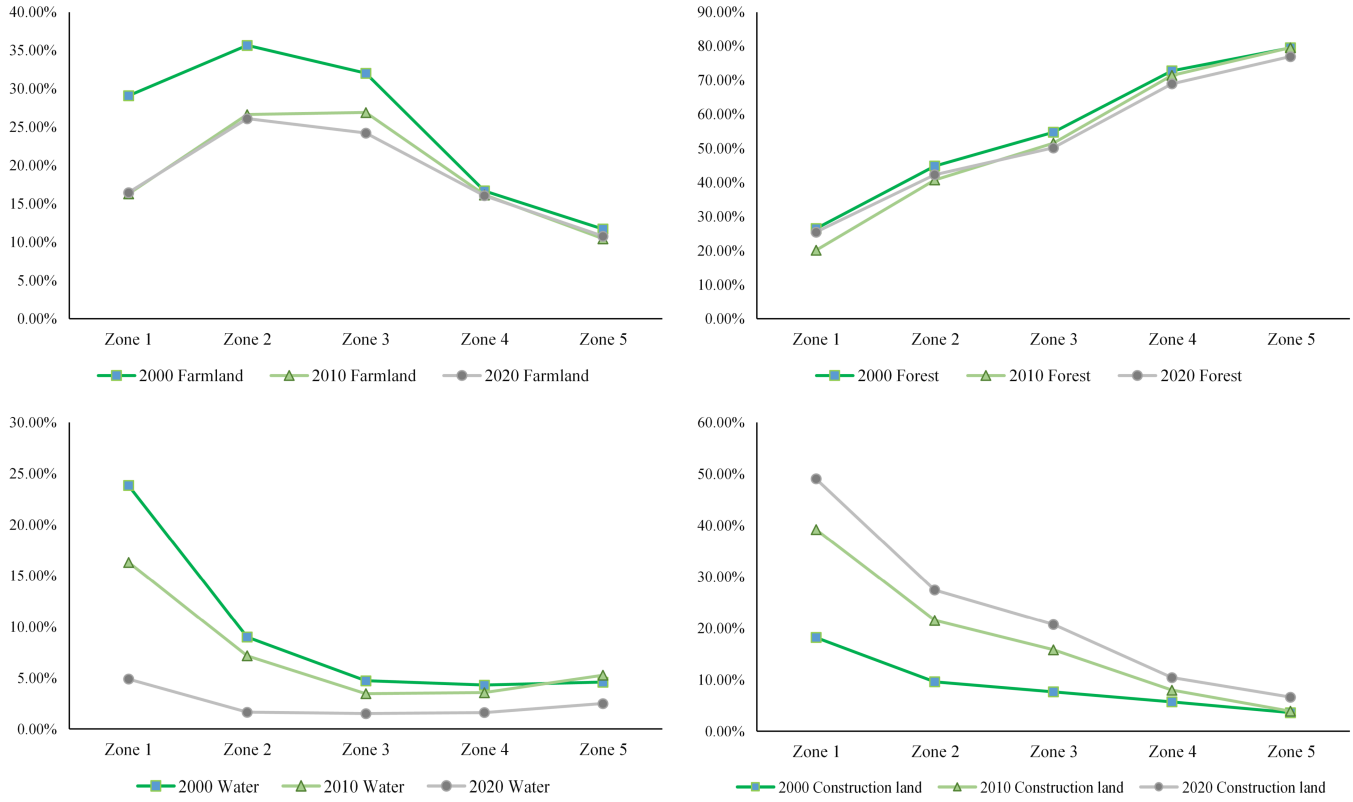


Figure 10. Changes in the ecosystem service value proportion of farmland, forest, water, and construction land.

Land use conversion processes and intensity are clearly depicted by the Sankey diagrams for each zone (Figure 11). Land activity intensity gradually decreased from Zone 1 to Zone 5 with increasing distance from the coastline. Forestland dominated Zones 4 and 5 and remained stable between 2000 and 2020. Extensive land use conversions occurred from Zone 1 to Zone 3, driven mainly by the expansion of construction land at the expense of farmland. From 2000 to 2010, large areas of the latter were converted to the former in Zones 1 and 2; however, this conversion slowed during 2010–2020. Unlike Zone 2, Zone 1 also experienced considerable conversion of water bodies to construction land. From 2000 to 2010, water bodies in Zone 1 were mainly converted to construction land and barren land; from 2010 to 2020, they continued to be developed for construction, and most barren land was also converted.

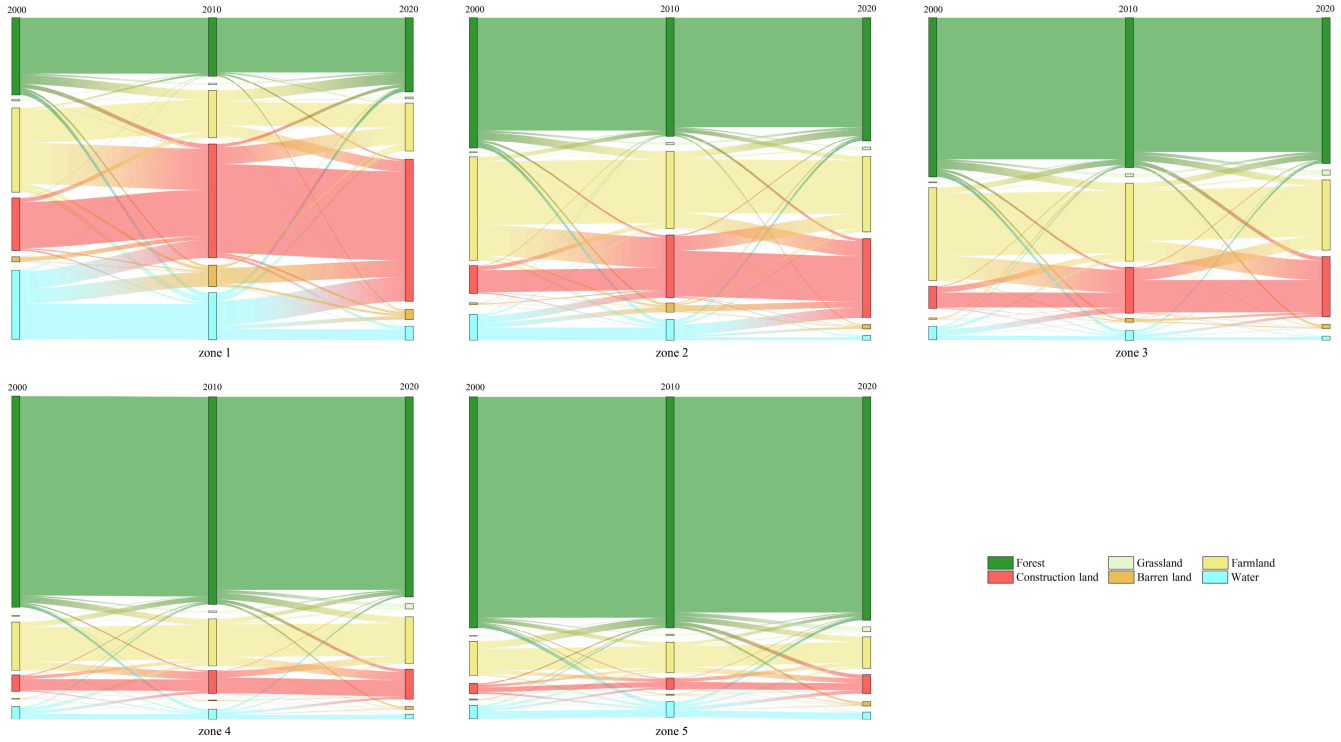


Figure 11. Sankey diagram for each zone from 2000 to 2020.

3.2.2. Robustness Test of Land–Sea Gradient Zoning and Spatiotemporal Differentiation of Ecosystem Service Value

(1) Zoning Robustness Test

The statistical results of the ESV loss rates under different zoning schemes (Table 5) show the following: under the three-zone scheme, the ESV reduction rates of the first and second nearshore gradients were 72.82% and 18.10%, respectively, together accounting for 90.92%; under the five-zone scheme, the gradients together accounted for approximately 80%; under the seven-zone scheme, the ESV reduction rates of the gradients were 39.63% and 27.61%, respectively, together accounting for 67.23%. Regardless of the zoning scheme adopted, ESV losses were consistently highly concentrated in the nearshore area, and the core spatial pattern remained stable, indicating that the number of gradient zones does not alter the principal conclusion of this study—that ESV loss is concentrated in the nearshore area—and that the five-zone scheme exhibits sufficient robustness.

Table 5. Robustness test of ESV loss share of different zone gradient schemes.

	Three-Zone	Five-Zone	Seven-Zone
Zone 1	72.82%	56.61%	39.63%
Zone 2	18.10%	22.59%	27.61%
Zone 3	9.08%	10.60%	11.77%
Zone 4	-	6.83%	8.63%
Zone 5	-	3.37%	5.55%
Zone 6	-	-	4.96%
Zone 7	-	-	1.86%
Total	100.00%	100.00%	100.00%

(2) Gradient Differentiation Characteristics of Total ESV

From 2000 to 2020, the ESV exhibited a distinct gradient pattern characterized by significant nearshore losses and stable offshore conditions. The ESV in Zone 1 plummeted

from 15,362.42 × 10^5 yuan to 5035.31 × 10^5 yuan, representing a loss rate of 67.2%, which is much higher than the island-wide average of 43.3%. Approximately 80% of the total ESV loss was concentrated in Zones 1 and 2, suggesting that the nearshore area was the core zone of ecosystem service degradation. In contrast, Zone 4, where forestland covered more than 65% of the area, showed a low ESV loss rate of 19%, serving as a key zone supporting ecological stability across the island.

(3) Gradient Differentiation Characteristics of ESV Service Functions

Shifts in ecosystem service functions varied noticeably across zones, with an overall declining trend from 2000 to 2020 (Figure 12). Regulating services consistently remained the core function of the island ecosystem, with the most noticeable change being in Zone 1, where their value dropped from 12,997.82 × 10^5 yuan to 3927.72 × 10^5 yuan, a decrease of nearly 70%. Support services displayed significant spatial variation, with Zone 4 being a high-value area and Zone 1 comparatively lower. Provisioning services accounted for a relatively small proportion of total ESV but experienced a drastic decline; their value in Zone 1 decreased from 1072.05 × 10^5 yuan to 320.16 × 10^5 yuan, representing a substantial reduction of 70.1%, the most prominent relative loss among all gradient zones. Cultural services accounted for the smallest proportion, and their total value remained generally stable.

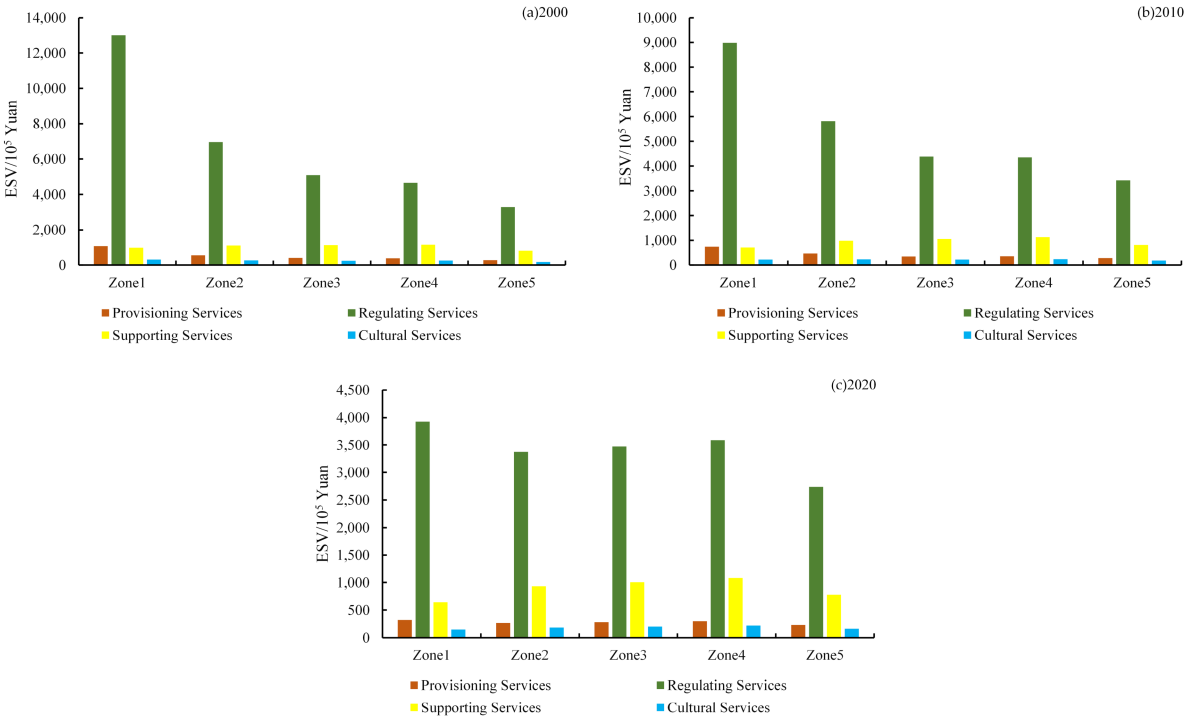


Figure 12. Ecosystem individual service value for each zone from 2000 to 2020.

4. Discussion

4.1. Land–Sea Gradient Pattern, Driving Mechanisms, and Ecological Degradation Pressure

Using the five delineated zones as sample points, Spearman's rank correlation coefficient was employed to quantitatively examine the monotonic relationship between the comprehensive land use dynamic degree and the mean distance from the coastline. The results for both periods reveal a statistically significant monotonic negative correlation (2000–2010: $\rho = -1.000$, $p < 0.05$; 2010–2020: $\rho = -1.000$, $p < 0.05$) (Figure 13), indicating that the intensity of land use change exhibited a systematic declining trend from the coastline inland.

However, further comparison of the dynamic degree values between the two periods reveals that subtle internal adjustments occurred within this distance–decay pattern. The

nearshore zones (Zone 1–2) exhibited a decelerating trend. During 2000–2010, the dynamic degree of Zone 1, closest to the coast, was as high as 2.05% and decreased to 1.90%, and that of Zone 2 also slightly declined from 1.36% to 1.33%. This reflects that, following the initial phase of rapid development, available land resources in nearshore areas have become increasingly constrained, and development intensity has gradually approached saturation. In contrast, the offshore zones (Zone 4–5) exhibited an accelerating trend. The degrees of Zones 4 and 5 increased from 0.68% to 0.76%, and from 0.61% to 0.70%, respectively, indicating that hotspots of land use change are migrating inland with increasing distance from the coast.

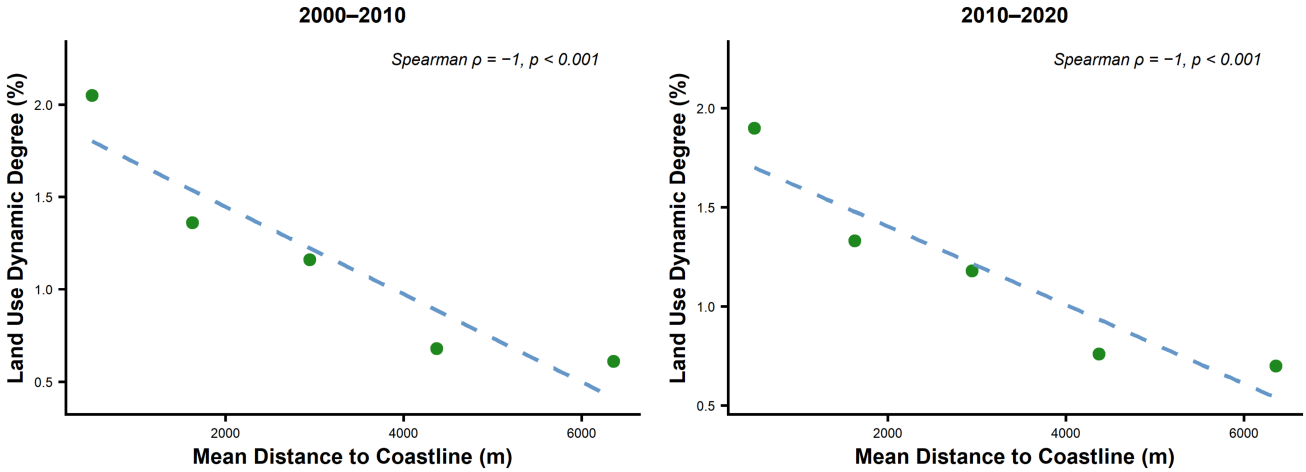


Figure 13. Monotonic decline of land use intensity with distance from coastline: Spearman's rank correlation results.

The above differentiation pattern of "nearshore deceleration and offshore acceleration," while maintaining the overall distance–decay pattern, reveals an inlandward shift in the spatial center of land use change. Although the Spearman rank correlation coefficient remained at a highly significant monotonic level of −1.000 in both periods, a reciprocal shift between nearshore and offshore zones is evident at the numerical level.

Zhoushan City is a typical island city with a highly developed marine economy. In 2021, Zhoushan's gross ocean product reached 116 billion yuan, accounting for 68% of its GDP, one of the highest proportions in the country. From 2000 to 2020, its leading industry gradually shifted from traditional agriculture and fisheries to non-agricultural industries, including port logistics, coastal industries, and marine tourism [56]. As a typical island port city with a proportionally large marine economy and strong drivers of urbanization, Zhoushan's gradient pattern exhibits both commonalities and unique characteristics.

As shown in Figure 13, the land use intensity of Zhoushan Island decreased with increasing distance from the coast. Early coastal development was much stronger than inland development; however, the differences between zones gradually narrowed in the later period, and development tended to be balanced, consistent with the evolutionary patterns of port cities such as Yantai [27]. Yet, Zhoushan Island also has special traits.

First, 43% of urban expansion (the increase in the proportion of construction land) occurred in Zone 1, which is within 1 km of the coastline, leading to more clustered development, steeper gradients, and more localized ecological impacts, and thus differentiating it from mainland coastal areas. Second, the transfer of cultivated land to construction land showed a phased spatial migration, beginning nearshore in Zones 1–2 and later moving toward Zone 3, due to the shrinkage of coastal cultivated land. Third, because of sea reclamation projects focused on Zone 1 and nearshore waters, a clear chain conversion of

"water body → unused land → construction land" was observed during the study period, revealing the gradual encroachment of sea reclamation on the island's ecological space.

Zhoushan's urbanization and industrialization have come at the expense of tidal-flat reclamation, loss of arable land, and wetland loss. In 2020, the ESV was only 56.7% of its 2000 level, with the largest declines in regulating and provisioning services. The weakening of regulatory services has led to the deterioration of the ecological environment and increased vulnerability to natural hazards, and the continued decline in provisioning services has also exerted a significant impact on regional grain production (see Section 4.2.3 for details). The above results indicate that intensive coastal development activities, while driving economic growth, have imposed non-negligible degradation pressure on the long-term sustainability of the island ecosystem.

4.2. Policy Implications, Limitations, and Recommendations

4.2.1. Sea Reclamation Policy: Development-Driven and Ecological Costs

In recent years, China's rapid economic development has intensified disturbances to coastal ecosystems. Sea reclamation is one of the main drivers of ecological degradation of coastal ecosystems, which manifests as reduced biodiversity and bird habitats [57–60]. Furthermore, ESV exhibits a significant negative correlation with the intensity of sea reclamation [61,62]. Empirical evidence has confirmed that the reduction in water areas and wetland habitats caused by sea reclamation is the primary driver of the decline in ESV [63–65].

As an island city, Zhoushan has experienced rapid population growth and faces extreme scarcity of land resources. The reclamation projects in Zhejiang Province have a long history [64]: since 1990, Zhoushan City has implemented large-scale sea reclamation projects, including Putuo Donggang Reclamation Project, Zhoushan Diaoliang Reclamation Project, and Southeast Lujiazhi Shoal Reclamation Project, etc. The spatial distribution of these major reclamation projects shows a high degree of overlap with the "water → barren → construction" conversion zones identified in this study (Figure 14, Table 6), providing direct spatial evidence that reclamation-driven land conversion is the primary cause of nearshore ESV loss. The national and Zhejiang Province governments have issued several policies encouraging sea reclamation, including the "National Marine Economic Development Plan Outline" and "the Overall Plan for Tidal Flat Reclamation in Zhejiang Province (2005–2020)", allowing reclaimed land to be used as supplementary arable land, which directly promoted large-scale sea reclamation in Zhoushan. From 2005 to 2020, 26 sea reclamation projects were planned in Zhoushan, totaling 14,860 ha, providing substantial land for urbanization, industrialization, and marine economic development, but also leading to ESV decline, reduced biodiversity, and degradation of tidal flat ecosystems.

Table 6. Major coastal reclamation projects on Zhoushan Island.

No.	Project Name	Implementation Period
1	Dongdatang Outer Shoal Reclamation Project	2010–2020
2	Zikutu Outer Shoal Reclamation Project	2000–2010
3	Southeast Lujiazhi Shoal Reclamation Project	2010–2020
4	Zhoushan Diaolang Reclamation Project	2000–2010
5	Zhoushan Diaoliang Reclamation Project	2010–2020
6	Putuo Donggang Reclamation Project	2000–2010

Since 2018, the government has tightened restrictions on sea reclamation, stopping approval of new projects except for major national strategic ones, thereby effectively limiting large-scale reclamation. However, the policy has clear delays and shortcomings, and long-term sea reclamation has caused permanent harm to the nearshore ecosystem.

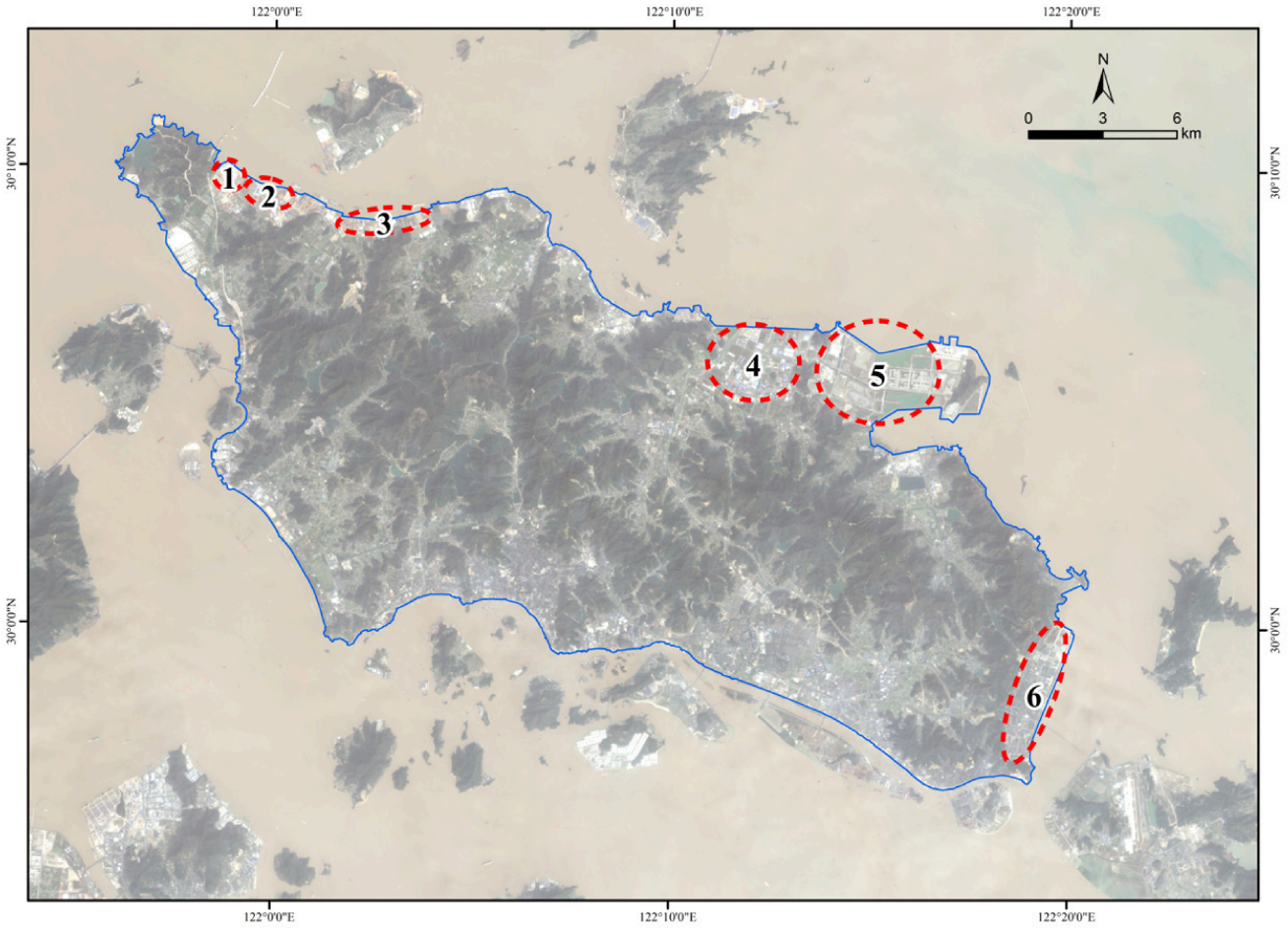


Figure 14. Spatial distribution of major coastal reclamation projects on Zhoushan Island (2000–2020). The numbers in the figure correspond to the "No." column in Table 6, indicating the same reclamation projects.

4.2.2. Soil and Water Conservation Policy: Effectiveness and Shortcomings

During the study period, the forestland area in Zhoushan City remained relatively stable overall. The rate of converting cultivated land to forestland in the latter period was significantly higher than the reverse transformation of forestland, mainly due to the ongoing efforts to return farmland to forest and soil and water conservation projects in the area. In recent years, China has developed and implemented a series of special soil and water conservation policies to tackle soil erosion issues [66,67]. As a long-term area for these policies, Zhoushan City, despite facing challenges such as heavy rainfall, strong winds, typhoons, and a high risk of geological disasters, has effectively used soil and water conservation measures to curb regional ecological degradation and maintain local ecological security. However, there are still clear shortcomings in the current soil and water conservation policies: on the one hand, policy efforts mainly focus on protecting forest land, with insufficient attention paid to key ecosystems such as tidal flats, wetlands, and water bodies; on the other hand, policies have yet to establish an effective coordination mechanism with related areas such as urban expansion control and sea reclamation management.

4.2.3. Urban Planning and Food Security: Lagged Governance and Growing Security Risks

Based on data from the Zhoushan Statistical Yearbook 2021, the total grain output of Zhoushan City dropped from 88,000 tons in 2000 to 29,000 tons in 2020, a decline of 67%. According to the remote sensing interpretation results of this study, the farmland area on Zhoushan Island decreased from 14,054 hectares to 10,277 hectares over the same period, a reduction of 26.9%. The substantially larger decline in grain output compared

with the reduction in farmland area indicates that, in addition to the loss of cultivated land, changes in cropping structure were also an important factor contributing to the decrease in grain production. As an island city connected to the mainland only by sea-crossing bridges, Zhoushan's grain self-sufficiency rate has fallen below 10%, meaning it must highly dependent on external supplies and is facing sustained food security pressure beyond its own carrying capacity.

Spatially, farmland loss was concentrated mainly in the nearshore Zone 1 and Zone 2, driven primarily by the large-scale conversion of farmland to construction land, which not only directly reduced the land area available for grain production but also exacerbated the fragmentation of the agricultural landscape, further undermining yield stability.

Although the latest territorial spatial plan (2024) emphasizes the importance of protecting farmland and ensuring food security, the policy response has shown a noticeable lag. Long-term high-intensity development has substantially reduced farmland area and led to the continuous degradation of ecosystem services. Relying solely on short-term planning and regulation is insufficient to rapidly reverse the ecological degradation pressure that has accumulated over the long term.

4.3. Comparison with Related Studies

Numerous scholars have conducted research on land use and ecosystem service value in the Zhoushan Archipelago. The findings of this study are generally consistent with those of Shao et al. (2017) and Xi et al. (2021) [34,36]: all research indicates rapid expansion of construction land, reduction in farmland and coastal wetland water areas, and a consequent overall decline in ecosystem service value. Specifically, Shao et al. (2017), focusing on the Dinghai District of Zhoushan, concluded that urban expansion and the sharp reduction in tidal flat wetlands led to a continuous decline in ESV, which is entirely consistent with the declining trend observed in this study [36]. Xi et al. (2021), in their study of ESV across the entire Zhoushan Archipelago from 2000 to 2020, similarly identified an overall pattern of decline [34].

A directional difference exists between the findings of this study and those of [37], who reported a 13.46% increase in total ESV for the entire Zhoushan Archipelago from 1984 to 2017. This discrepancy arises primarily from three key differences in study design: (1) Study extent: This study focused on Zhoushan Island and its nearshore reclamation areas, where human disturbances are concentrated and ecological degradation is prominent, whereas [37] covered the entire Zhoushan Archipelago, where the stable ecological background of outlying islands and open waters diluted the declining trend observed on the main island. (2) Study period: This study focused on the period of intensive development from 2000 to 2020, a critical stage of rapid ESV decline, whereas [37] included the period from 1984 to 2000, when development intensity was relatively low, which elevated the overall magnitude of change over the longer time series. (3) Shoreline baseline: This represents the most fundamental methodological difference. [37] adopted a year-by-year dynamic shoreline, whereby artificial water bodies such as aquaculture ponds created through reclamation were classified as water area, masking the ecological degradation of the original marine waters. In contrast, this study adopted the fixed 2020 shoreline, directly accounting for the conversion of natural water bodies to barren land and construction land as ecological loss, thereby more realistically reflecting the encroachment upon and destruction of the original marine ecosystem by reclamation.

In summary, the differences in conclusions between this study and [37] are essentially the reasonable result of differing study extents, time periods, and shoreline baseline settings. The fixed-shoreline approach adopted in this study is more suitable for revealing the ecological costs borne by islands that serve as core areas of reclamation. Together with studies employing

dynamic shorelines, these approaches complement one another and collectively enrich the multi-scale understanding of ecological changes in the Zhoushan Archipelago.

4.4. Implications for Management Practice

In response to the dynamic changes in the ecological service value of Zhoushan Island and the accompanying management challenges, we propose four targeted recommendations: (1) It is imperative to fully recognize the unique natural, geographic, and ecological characteristics of the islands and to implement tailored, differentiated management policies. Simultaneously, improving coordination among various regulatory measures will enhance overall coherence and strategic alignment. (2) Delays in urban planning impede prompt responses to issues arising from rapid urbanization, land reclamation, and ecological shifts in island cities. Therefore, establishing a dynamically updated planning framework that incorporates land–sea coordination is essential to improve scientific accuracy and foresight, thereby reducing ecological and spatial risks associated with planning delays. (3) Although strict controls and restrictions on land reclamation are in place, comprehensive and cautious ecological risk assessments should be conducted for all new projects. Approval standards and development intensities must be rigorously regulated to prevent adverse impacts on island ecosystems, coastal wetlands, and biodiversity. (4) To mitigate the ecological degradation and functional decline resulting from historical development, systematic and quantitative ecological impact assessments should be conducted. Such assessments would help identify damaged areas, ecological corridors, and vulnerable zones, thereby supporting the gradual restoration of regional ecological functions and the long-term sustainability of the ecosystem.

4.5. Limitations and Prospects

This study, based on land use data from 2000 to 2020, revealed the spatiotemporal changes in ecosystem service value (ESV) and its land–sea gradient differentiation characteristics on Zhoushan Island. However, certain limitations remain.

(1) Limitations of the land use classification system.

This study adopted the commonly used first-level land use classification system. Constrained by the 30 m spatial resolution of Landsat imagery, it did not conduct fine-scale differentiation between natural water bodies and artificial aquaculture ponds, or between natural tidal flats and reclaimed bare land. Coastal wetland types such as salt pans, tidal flats, and aquaculture ponds were uniformly grouped into the water body category, resulting in insufficient precision in representing the internal structure of ESV. Future research could establish a more refined second-level classification system, separately delineating aquaculture ponds, salt pans, and artificial wetlands, and applying differentiated ecological value equivalent coefficients to more accurately characterize the ecological functional differences among various coastal land use types.

(2) Limitations of the ecosystem service assessment.

In this study, only the island area and nearshore reclaimed zones were considered, without integrating adjacent marine ecological processes into the comprehensive analysis. In addition, although cultural services were included in the assessment framework, their value was estimated solely using the equivalent factor method, which cannot adequately reflect the actual cultural service value of Zhoushan as a marine tourism city. Future research could incorporate questionnaire surveys, visitor willingness-to-pay data, and ecotourism statistics to conduct more refined localized corrections of cultural service values. Meanwhile, adjacent marine ecological processes could be integrated into the analytical framework to achieve a more complete assessment of island and coastal ecosystem services.

(3) Limitations of the driving mechanism analysis.

This study employed macro-scale spatiotemporal remote sensing data, without delving into micro-scale ecological processes, localized human activities, or the dynamic impacts of climate change. The interactions and feedback mechanisms among various policy measures also remain to be quantitatively modeled. Future research could leverage the GEE platform to extend the time series of remote sensing data, couple the InVEST model with machine learning algorithms, and integrate multiple natural, social, and policy drivers to construct a multi-scale analytical framework for driving mechanisms. Simultaneously, quantifying policy synergy effects could provide more robust scientific support for island ecological conservation and sustainable coastal management.

5. Conclusions

Based on the GEE platform, Landsat remote sensing images from 2000, 2010, and 2020 were selected in this study and the Random Forest classification method was employed to extract six land use types on Zhoushan Island. By integrating the land use dynamic degree, transfer matrix, and ecosystem service value (ESV) assessment methods, the spatiotemporal evolution of land use on Zhoushan Island from 2000 to 2020 was systematically analyzed. Meanwhile, five land–sea gradient zones were delineated based on Euclidean distance from the coastline to reveal the spatial differentiation characteristics of land use change and ESV gains and losses, thereby providing a scientific basis for the sustainable development of the island. The main conclusions are as follows:

(1) Significant changes in land use pattern: From 2000 to 2020, Zhoushan Island exhibited an overall pattern of continuous reduction in water bodies and farmland alongside rapid expansion of construction land, driven by urbanization, industrial transformation, and policy regulation. A typical "water body $\rightarrow$ barren land $\rightarrow$ construction land" land conversion chain process was observed in localized areas, closely linked to nearshore reclamation activities.

(2) Persistent decline in ecosystem service value: Large-scale land use conversion led to a continuous decline in regional ESV, with the 2020 ESV amounting to only 56.7% of that in 2000. The decline in regulating and provisioning services was the most pronounced. The ESV net transfer matrix analysis revealed that the core driving force behind the ESV decline was the large-scale conversion of high-ecological-value water bodies to low-value construction land and barren land, with the magnitude of loss far exceeding the ecological gains generated by forest and grassland recovery.

(3) Mounting food security pressure: The reduction in farmland area, compounded by the shift toward non-grain cropping structures, resulted in a decline in grain output substantially exceeding the rate of farmland loss. Zhoushan's grain self-sufficiency rate has fallen below 10%, leaving it highly dependent on external supplies and facing sustained food security pressure beyond its own carrying capacity. Although the latest territorial spatial plan has delineated farmland and ecological protection bottom lines, the policy response has exhibited a noticeable lag.

(4) Pronounced land–sea gradient differentiation: Both the intensity of land use change and ESV loss exhibited a progressive decline from the nearshore to the inland zones. Nearshore Zones 1 and 2 experienced the most intensive land use conversions, jointly contributing approximately 80% of the total ESV loss. In contrast, Zones 4 and 5, with a higher proportion of forest cover, maintained relatively stable land use structures and stronger ecological support capacity. Spearman's rank correlation analysis confirmed a statistically significant monotonic decreasing relationship between land use dynamic degree and distance from the coastline. The overall spatial evolution pattern is similar to

that of other coastal port cities such as Yantai, reflecting the universal land–sea gradient differentiation characteristic of island urbanization processes.

(5) Policy and planning as the core driving force: Early reclamation policies promoted the rapid transformation of coastal land, while the subsequent tightening of reclamation controls effectively curbed disorderly expansion. Ecological projects such as returning farmland to forest also contributed to maintaining the relative stability of the forest landscape. Current island research tends to focus predominantly on ESV numerical accounting, with insufficient attention paid to land structure degradation and long-term ecological degradation pressure. Through a land–sea gradient perspective, this study systematically quantified the spatiotemporal evolution of land use and ESV on Zhoushan Island, revealing the differentiated response characteristics and driving mechanisms of ecosystems across different gradient zones. These findings provide empirical support for island territorial management, ecological conservation, and sustainable development planning, as well as a reference for similar island studies.

Supplementary Materials: The following supporting information can be downloaded at: https://www.mdpi.com/article/10.3390/su18115649/s1, Table S1: Confusion matrix of land use classification results; Table S2: Transfer matrix of ecosystem service value changes caused by land use conversion.

Author Contributions: Conceptualization, W.M.; methodology, W.M.; software, F.W.; validation, L.S.; resources, Y.T.; writing—original draft preparation, W.M.; writing—review and editing, F.W.; visualization, D.W. All authors have read and agreed to the published version of the manuscript.

Funding: This research was funded by the Scientific Research Fund of the Second Institute of Oceanography, Ministry of Natural Resources, grant numbers JG2217 and JG2110.

Institutional Review Board Statement: Not applicable.

Informed Consent Statement: Not applicable.

Data Availability Statement: The datasets generated and analyzed during the current study are included in this published article.

Conflicts of Interest: The authors declare no conflicts of interest.

Abbreviations

The following abbreviations are used in this manuscript:

ESV	Ecosystem Service Value
LUCC	Land Use/Cover Change
GEE	Google Earth Engine

References

1. Guida-Johnson, B.; Zuleta, G.A. Land-use land-cover change and ecosystem loss in the Espinal ecoregion, Argentina. *Agric. Ecosyst. Environ.* **2013**, *181*, 31–40. [CrossRef]
2. He, C.; Shao, H.; Xian, W. Spatiotemporal Variation and Driving Forces Analysis of Eco-System Service Values: A Case Study of Sichuan Province, China. *Int. J. Environ. Res. Public Health* **2022**, *19*, 8595. [CrossRef]
3. Yan, F.; Zhang, S.; Liu, X.; Chen, D.; Chen, J.; Bu, K.; Yang, J.; Chang, L. The Effects of Spatiotemporal Changes in Land Degradation on Ecosystem Services Values in Sanjiang Plain, China. *Remote Sens.* **2016**, *8*, 917. [CrossRef]
4. Costanza, R.; d'Arge, R.; De Groot, R.; Farber, S.; Grasso, M.; Hannon, B.; Limburg, K.; Naeem, S.; O'Neill, R.V.; Paruelo, J.; et al. The value of ecosystem services: Putting the issues in perspective. *Ecol. Econ.* **1998**, *25*, 67–72. [CrossRef]
5. Sannigrahi, S.; Bhatt, S.; Rahmat, S.; Paul, S.K.; Sen, S. Estimating global ecosystem service values and its response to land surface dynamics during 1995–2015. *J. Environ. Manag.* **2018**, *223*, 115–131. [CrossRef] [PubMed]
6. Makwinja, R.; Curtis, C.J.; Tesfamichael, S.G. Rapidly declining wetland ecosystem service value indicated by land use/land cover changes in the Elephant Marsh, Malawi. *Ecol. Indic.* **2026**, *184*, 114726. [CrossRef]

7. Bekele, B.; Wei, W.; Tsegaye, L.; Tilahun, M.; Girma, T.; Ketema, H. Urban expansion-induced land use land cover changes and the subsequent changes in ecosystem service and land surface temperature in the central highland of Ethiopia. *Environ. Sustain. Indic.* **2025**, *26*, 100626. [CrossRef]
8. Corvalan, C.; Hales, S.; McMichael, A.J. *Ecosystems and Human Well-Being: Health Synthesis*; World Health Organization: Geneva, Switzerland, 2005.
9. Costanza, R.; d'Arge, R.; de Groot, R.; Farber, S.; Grasso, M.; Hannon, B.; Limburg, K.; Naeem, S.; O'Neill, R.V.; Paruelo, J.; et al. The value of the world's ecosystem services and natural capital. *Nature* **1997**, *387*, 253–260. [CrossRef]
10. Crossman, N.D.; Burkhard, B.; Nedkov, S.; Willemen, L.; Petz, K.; Palomo, I.; Drakou, E.G.; Martín-Lopez, B.; McPhearson, T.; Boyanova, K.; et al. A blueprint for mapping and modelling ecosystem services. *Ecosyst. Serv.* **2013**, *4*, 4–14. [CrossRef]
11. Costanza, R.; de Groot, R.; Sutton, P.; van der Ploeg, S.; Anderson, S.J.; Kubiszewski, I.; Farber, S.; Turner, R.K. Changes in the global value of ecosystem services. *Glob. Environ. Change* **2014**, *26*, 152–158. [CrossRef]
12. De Groot, R.; Brander, L.; van der Ploeg, S.; Costanza, R.; Bernard, F.; Braat, L.; Christie, M.; Crossman, N.; Ghermandi, A.; Hein, L.; et al. Global estimates of the value of ecosystems and their services in monetary units. *Ecosyst. Serv.* **2012**, *1*, 50–61. [CrossRef]
13. Xie, G.-d.; Lu, C.-X.; Leng, Y.-F.; Zheng, D.; Li, S.-C. Ecological assets valuation of the Tibetan Plateau. *J. Nat. Resour.* **2003**, *18*, 189–196.
14. Xie, G.-d.; Zhen, L.; Lu, C.-X.; Xiao, Y.; Chen, C. Expert knowledge based valuation method of ecosystem services in China. *J. Nat. Resour.* **2008**, *23*, 911–919.
15. Xie, G.; Zhang, C.; Zhen, L.; Zhang, L. Dynamic changes in the value of China's ecosystem services. *Ecosyst. Serv.* **2017**, *26*, 146–154. [CrossRef]
16. Macarthur, R.; Wilson, E. Equilibrium-Theory of Insular Zoogeography. *Evolution* **1963**, *17*, 373–387. [CrossRef]
17. MacArthur, R.H.; Wilson, E.O. *The Theory of Island Biogeography*; Princeton University Press: Princeton, NJ, USA, 2001; Volume 1.
18. Rick, T.C.; Radde, H.D.; Teeter, W.G.; Elliott Smith, E.A.; Alvitre, C.M.; Dagtas, N.D.; Kennedy-Richardson, K.O.; King, J.L.; Martinez, D.R.; Schnorr, S.; et al. Enhancing biodiversity: Historical ecology and biogeography of the Santa Catalina Island ground squirrel, Otospermophilus beecheyi nesioticus. *R. Soc. Open Sci.* **2024**, *11*, 240726. [CrossRef]
19. Jackson, A.C.; White, O.W.; Carine, M.; Chapman, M.A. The role of geography, ecology, and hybridization in the evolutionary history of Canary Island Descurainia. *Am. J. Bot.* **2023**, *110*, e16162. [CrossRef]
20. Kelman, I. Critiques of island sustainability in tourism. *Tour. Geogr.* **2019**, *23*, 397–414. [CrossRef]
21. Kurniawan, F.; Adrianto, L.; Bengen, D.G.; Prasetyo, L.B. Vulnerability assessment of small islands to tourism: The case of the Marine Tourism Park of the Gili Matra Islands, Indonesia. *Glob. Ecol. Conserv.* **2016**, *6*, 308–326. [CrossRef]
22. Wibisono, M.G.; Asdak, C.; Wawan; Dwiratna, S. Unlocking the sustainability potential of Liberica coffee (Coffea liberica) in Riau's tropical peatlands: Strategic insights from Rangsang Island, Indonesia. *Sustain. Futures* **2025**, *10*, 101187. [CrossRef]
23. Guimarães, M.H.; Ballé-Béganton, J.; Bailly, D.; Newton, A.; Boski, T.; Dentinho, T. Transdisciplinary conceptual modeling of a social-ecological system—A case study application in Terceira Island, Azores. *Ecosyst. Serv.* **2013**, *3*, e22–e31. [CrossRef]
24. Durap, A. Beachface steepness modulates erosion but not recovery: Multi-decadal spatiotemporal shoreline evidence across 390 transects. *J. Sea Res.* **2025**, *208*, 102644. [CrossRef]
25. Durap, A. Multi-decadal spatiotemporal shoreline vulnerability assessment (1987–2025): Integrating erosion-accretion dynamics for disaster risk reduction across 90 coastal transects. *Nat. Hazards* **2025**, *121*, 22981–23019. [CrossRef]
26. Hou, X.; Xu, X. Spatial patterns of land use in coastal zones of China in the early 21st century. *Geogr. Res.* **2011**, *30*, 1370–1379.
27. Yan, J.; Xiao, R.; Su, F.; Bai, J.; Jia, F. Impact of Port Construction on the Spatial Pattern of Land Use in Coastal Zones Based on CLDI and LUT Models: A Case Study of Qingdao and Yantai. *Remote Sens.* **2021**, *13*, 3110. [CrossRef]
28. Magarotto, M.G.; da Costa, M.F.; Tenedório, J.A.; Silva, C.P. Vertical growth in a coastal city: An analysis of Boa Viagem (Recife, Brazil). *J. Coast. Conserv.* **2015**, *20*, 31–42. [CrossRef]
29. Xie, Z.; Li, X.; Chi, Y.; Jiang, D.; Zhang, Y.; Ma, Y.; Chen, S. Ecosystem service value decreases more rapidly under the dual pressures of land use change and ecological vulnerability: A case study in Zhujiajian Island. *Ocean Coast. Manag.* **2021**, *201*, 105493. [CrossRef]
30. Yetein, M.H.; Houessou, L.G.; Amadou Siako, A.S.; Gbodja, G.T.; Oumorou, M. The impacts of land use/land cover changes on ecosystem service values in coastal lagoon landscapes of the 1017 Ramsar site, Benin. *Sci. Afr.* **2025**, *28*, e02695. [CrossRef]
31. Chen, C.; Liang, J.; Xie, F.; Hu, Z.; Sun, W.; Yang, G.; Yu, J.; Chen, L.; Wang, L.; Wang, L.; et al. Temporal and spatial variation of coastline using remote sensing images for Zhoushan archipelago, China. *Int. J. Appl. Earth Obs. Geoinf.* **2022**, *107*, 102711. [CrossRef]
32. Cao, W.; Li, R.; Chi, X.; Chen, N.; Chen, J.; Zhang, H.; Zhang, F. Island urbanization and its ecological consequences: A case study in the Zhoushan Island, East China. *Ecol. Indic.* **2017**, *76*, 1–14. [CrossRef]
33. Zhang, H.; Xiao, Y. Planning island sustainable development policy based on the theory of ecosystem services: A case study of Zhoushan Archipelago, East China. *Isl. Stud. J.* **2019**, *15*, 237–252. [CrossRef]
34. Xi, H.; Cui, W.; Cai, L.; Chen, M.; Xu, C. Evaluation and Prediction of Ecosystem Service Value in the Zhoushan Islands Based on LUCC. *Sustainability* **2021**, *13*, 2302. [CrossRef]

35. Liu, M.; Zhao, S. Spatial Assessment of Ecosystem Services in Zhoushan Archipelago Based on InVEST Model. *Sustainability* **2025**, *17*, 3913. [CrossRef]
36. Shao, X.; Jing, C.; Qi, J.; Jiang, J.; Liu, Q.; Cai, X. Impacts of land use and planning on island ecosystem service values: A case study of Dinghai District on Zhoushan Archipelago, China. *Ecol. Process.* **2017**, *6*, 27. [CrossRef]
37. Wang, L.; Chen, C.; Xie, F.; Hu, Z.; Zhang, Z.; Chen, H.; He, X.; Chu, Y. Estimation of the value of regional ecosystem services of an archipelago using satellite remote sensing technology: A case study of Zhoushan Archipelago, China. *Int. J. Appl. Earth Obs. Geoinf.* **2021**, *105*, 102616. [CrossRef]
38. Chen, J.; Pan, D.; Mao, Z.; Chen, N.; Zhao, J.; Liu, M. Land-cover reconstruction and change analysis using multisource remotely sensed imageries in Zhoushan Islands since 1970. *J. Coast. Res.* **2014**, *30*, 272–282. [CrossRef]
39. Dou, P.; Han, Z. Quantifying Land Use/Land Cover Change and Urban Expansion in Dongguan, China, From 1987 to 2020. *IEEE J. Sel. Top. Appl. Earth Obs. Remote Sens.* **2022**, *15*, 201–209. [CrossRef]
40. Ding, Y.; Yang, X.; Jin, H.; Wang, Z.; Liu, Y.; Liu, B.; Zhang, J.; Liu, X.; Gao, K.; Meng, D. Monitoring Coastline Changes of the Malay Islands Based on Google Earth Engine and Dense Time-Series Remote Sensing Images. *Remote Sens.* **2021**, *13*, 3842. [CrossRef]
41. Duan, Y.; Li, X.; Zhang, L.; Liu, W.; Liu, S.A.; Chen, D.; Ji, H. Detecting spatiotemporal changes of large-scale aquaculture ponds regions over 1988–2018 in Jiangsu Province, China using Google Earth Engine. *Ocean Coast. Manag.* **2020**, *188*, 105144. [CrossRef]
42. Sun, Z.; Luo, J.; Yang, J.; Yu, Q.; Zhang, L.; Xue, K.; Lu, L. Nation-Scale Mapping of Coastal Aquaculture Ponds with Sentinel-1 SAR Data Using Google Earth Engine. *Remote Sens.* **2020**, *12*, 3086. [CrossRef]
43. DeVries, B.; Huang, C.; Armston, J.; Huang, W.; Jones, J.W.; Lang, M.W. Rapid and robust monitoring of flood events using Sentinel-1 and Landsat data on the Google Earth Engine. *Remote Sens. Environ.* **2020**, *240*, 111664. [CrossRef]
44. Ning, J.; Liu, J.; Kuang, W.; Xu, X.; Zhang, S.; Yan, C.; Li, R.; Wu, S.; Hu, Y.; Du, G.; et al. Spatiotemporal patterns and characteristics of land-use change in China during 2010–2015. *J. Geogr. Sci.* **2018**, *28*, 547–562. [CrossRef]
45. Nasiri, V.; Deljouei, A.; Moradi, F.; Sadeghi, S.M.M.; Borz, S.A. Land Use and Land Cover Mapping Using Sentinel-2, Landsat-8 Satellite Images, and Google Earth Engine: A Comparison of Two Composition Methods. *Remote Sens.* **2022**, *14*, 1977. [CrossRef]
46. Tucker, C.J. Red and photographic infrared linear combinations for monitoring vegetation. *Remote Sens. Environ.* **1979**, *8*, 127–150. [CrossRef]
47. McFeeters, S.K. The use of the Normalized Difference Water Index (NDWI) in the delineation of open water features. *Int. J. Remote Sens.* **2007**, *17*, 1425–1432. [CrossRef]
48. Xu, H. Modification of normalised difference water index (NDWI) to enhance open water features in remotely sensed imagery. *Int. J. Remote Sens.* **2007**, *27*, 3025–3033. [CrossRef]
49. Bramhe, V.; Ghosh, S.K.; Garg, P.K. Extraction of built-up area by combining textural features and spectral indices from landsat-8 multispectral image. *Int. Arch. Photogramm. Remote Sens. Spat. Inf. Sci.* **2018**, *42*, 727–733. [CrossRef]
50. Yu, H.; Chen, C.; Shao, C. Spatial and temporal changes in ecosystem service driven by ecological compensation in the Xin'an River Basin, China. *Ecol. Indic.* **2023**, *146*, 109798. [CrossRef]
51. Ding, Z.; Su, F.; Zhang, J.; Zhang, Y.; Luo, S.; Tang, X. Clustering Coastal Land Use Sequence Patterns along the Sea–Land Direction: A Case Study in the Coastal Zone of Bohai Bay and the Yellow River Delta, China. *Remote Sens.* **2019**, *11*, 2024. [CrossRef]
52. Pan, F.; Shu, N.; Wan, Q.; Huang, Q. Land Use Function Transition and Associated Ecosystem Service Value Effects Based on Production–Living–Ecological Space: A Case Study in the Three Gorges Reservoir Area. *Land* **2023**, *12*, 391. [CrossRef]
53. Dark, S.; Bram, D. The modifiable areal unit problem (MAUP) in physical geography. *Prog. Phys. Geogr.* **2007**, *31*, 471–479. [CrossRef]
54. Tuson, M.; Yap, M.; Kok, M.R.; Murray, K.; Turlach, B.; Whyatt, D. Incorporating geography into a new generalized theoretical and statistical framework addressing the modifiable areal unit problem. *Int. J. Health Geogr.* **2019**, *18*, 6. [CrossRef] [PubMed]
55. Fotheringham, A.S.; Wong, D.W. The modifiable areal unit problem in multivariate statistical analysis. *Environ. Plan. A* **1991**, *23*, 1025–1044. [CrossRef]
56. Qiu, S.; Yue, W.; Zhang, H.; Qi, J. Island ecosystem services value, land-use change, and the National New Area Policy in Zhoushan Archipelago, China. *Isl. Stud. J.* **2017**, *12*, 177–198. [CrossRef]
57. Ji, X.; Xia, S.; Zhou, L. Impacts of reclamation and aquaculture on the wintering waterbird assemblage at a floodplain lakeshore based on multidimensional diversity. *Glob. Ecol. Conserv.* **2024**, *51*, e02926. [CrossRef]
58. Wang, C.; Xia, S.; Duan, H.; Wu, Y.; Su, Y.; Wang, B.; Shen, Z.; Sun, G.; Dong, B. Study on the impact of reclamation and development of Yancheng coastal wetlands on the spatio-temporal evolution of wintering Anatidae habitat. *Ecol. Indic.* **2024**, *160*, 111892. [CrossRef]
59. Chee, S.Y.; Tan, M.L.; Tew, Y.L.; Sim, Y.K.; Yee, J.C.; Chong, A.K.M. Between the devil and the deep blue sea: Trends, drivers, and impacts of coastal reclamation in Malaysia and way forward. *Sci. Total Environ.* **2023**, *858*, 159889. [CrossRef]
60. Ai, J.; Chen, L.; He, H.; Han, X. Revealing the long-term impacts of plant invasion and reclamation on native saltmarsh vegetation in the Yangtze River estuary using multi-source time series remote sensing data. *Ecol. Eng.* **2024**, *208*, 107362. [CrossRef]

61. Deng, J.; Lin, Y.; Zhou, M.; Wu, C.; Chen, B.; Xiao, G.; Cai, J. Ecosystem services dynamics response to tremendous reclamation in a coastal island city. *Ecosyst. Health Sustain.* **2019**, *5*, 155–168. [CrossRef]
62. Liu, R.; Xu, H.; Li, J.; Pu, R.; Sun, C.; Cao, L.; Jiang, Y.; Tian, P.; Wang, L.; Gong, H. Ecosystem service valuation of bays in East China Sea and its response to sea reclamation activities. *J. Geogr. Sci.* **2020**, *30*, 1095–1116. [CrossRef]
63. Zhao, B.; Kreuter, U.; Li, B.; Ma, Z.; Chen, J.; Nakagoshi, N. An ecosystem service value assessment of land-use change on Chongming Island, China. *Land Use Policy* **2004**, *21*, 139–148. [CrossRef]
64. Tian, P.; Li, J.; Cao, L.; Pu, R.; Gong, H.; Liu, Y.; Zhang, H.; Chen, H. Impacts of reclamation derived land use changes on ecosystem services in a typical gulf of eastern China: A case study of Hangzhou bay. *Ecol. Indic.* **2021**, *132*, 108259. [CrossRef]
65. Shan, J.; Li, J. Valuing marine ecosystem service damage caused by land reclamation: Insights from a deliberative choice experiment in Jiaozhou Bay. *Mar. Policy* **2020**, *122*, 104249. [CrossRef]
66. Liu, L.; Di, B.; Zhang, M. The tradeoff between ecological protection and economic growth in China's county development: Evidence from the soil and water conservation projects during 2011–2015. *Resour. Conserv. Recycl.* **2020**, *156*, 104745. [CrossRef]
67. Yang, Y.; Huang, L.; Deng, S.; Zhang, X.; Hou, W.; Xiao, S.; Shen, R.; You, X.; Yang, Y.; Pan, H. Tradeoffs among ecosystem services under ecological engineering construction: Donor and receiver evaluation of 25 soil and water conservation projects in China. *Ecol. Eng.* **2025**, *219*, 107685. [CrossRef]

Disclaimer/Publisher's Note: The statements, opinions and data contained in all publications are solely those of the individual author(s) and contributor(s) and not of MDPI and/or the editor(s). MDPI and/or the editor(s) disclaim responsibility for any injury to people or property resulting from any ideas, methods, instructions or products referred to in the content.